Psychological Research of Early Career Scientists
2023, Vol. 2, No. 1

not peer reviewed
ORIGINAL RESEARCH ARTICLE

PRECS
Psychological Research of Early Career Scientists

Assessment of parahippocampal integrity to estimate Alzheimer's disease status in structural MRI using a Cortex-to-Sulcus-Ratio

Lena Waldraff, Jens c. Pruessner, Xiang Hu

Department of Psychology,
University of Konstanz, Germany

Parahippocampal structures are the first to be damaged by Alzheimer's disease (AD). Structural changes can be detected at predementia-phase of mild cognitive impairment (MCI). However, utility of parahippocampal integrity for early AD-detection is limited due to high anatomical variability, mainly determined by the collateral sulcus. Presenting the Cortex-to-Sulcus-Ratio (CSR) correcting for this variability, the current study takes a first step in validating a relative measurement of parahippocampal integrity cross-sectionally assessing AD-status. The CSR is assumed to be superior to standard parahippocampal volumes as it improves differentiation between parahippocampal integrity of older adults being cognitively normal (CN), MCI or AD. Contrasting CSR and absolute parahippocampal volumes derived from manually segmented brains, this was examined in a sample of 24 individuals aged between 58 and 80 years, categorised as CN, MCI or AD. Investigating which parahippocampal structures might be relevant for AD-detection, different cortical volumes were considered individually and combinedly. Descriptive comparisons supported the presumed superiority: a clearer distinction was possible and the assumed group-order of parahippocampal integrity was only maintained when looking at the CSR. Considering age as a covariate, these observations could be statistically verified by significant group*integrity-measure-interactions for the left perirhinal and entorhinal cortex and a combined measure of left parahippocampal structures. Although validation requires further research, results support the idea of including a measurement of sulcal enlargement when evaluating parahippocampal integrity in aging individuals. The CSR seems to be beneficial in estimating AD-status in cross-sectional structural magnetic resonance imaging as it overcomes weaknesses of absolute volumetric measurements.

Keywords: aging, Alzheimer's disease, collateral sulcus, mild cognitive impairment, parahippocampal gyrus, structural MRI

Alzheimer's disease (AD) is characterised by progressive dementia. Clinically it initially presents as mild cognitive impairment (MCI) followed by more severe deficits in several domains until a disability threshold is reached and traditional criteria for probable AD are met (McKhann et al., 1984, 2011). From a biological perspective, AD is characterised by a neurodegenerative pathology: accumulation of abnormal proteins causes neuronal loss (Raskin, Cummings, Hardy, Schuh & Dean, 2015; Schultz, del Tredici, & Braak, 2004). Histopathological findings suggest that the destructive process begins in the medial temporal lobe (MTL) – more precisely in perirhinal (PRC) and entorhinal cortex (EC), which are structures of the parahippocampal gyrus (PHG) (Braak & Braak, 1991; Braak, Braak & Bohl, 1993). Even before clinical symptoms manifest neuropathological changes can be detected at a cellular level (De Strooper & Karran, 2016) and as structural atrophy (De Ture & Dickerson, 2019; Jack et al., 2005). This delay in the onset of the cognitive correlates proposes that pathological effects only appear once a clinical threshold is crossed (Frisoni, Fox, Jack, Scheltens & Thompson, 2010).

The National Institute on Aging - Alzheimer's Association research framework defines the disease via its underlying pathology, which can be depicted using

This work originated from the Master thesis of Lena Waldraff. This study was sponsored by University of Konstanz research funds to Prof. Dr. Jens Pruessner. The authors declare no conflict of interest. Formatting based on a template by Brenton M. Wiernik (https://osf.io/t4eqp/; DOI 10.17605/OSF.IO/HSV6A).
Correspondence concerning this paper should be addressed to Prof. Dr. Jens Pruessner (jens.pruessner@uni-konstanz.de).

biomarkers in vivo (Jack et al., 2012, 2018). Although the framework is not yet intended for clinical practice, its biological orientation, and efforts to find biomarkers pave the way for diagnosis in preclinical AD-phases and accede to individualised risk profiling for MCI- patients (Ebenau et al., 2020; van Maurik et al., 2019). As stated by Frisoni et al. (2017), biomarkers are important for detecting AD, but their development and use remain challenging. They recommend validating AD-biomarkers according to a five-phase framework. Against that background Ten Kate and colleagues (2017) evaluated whether MTL atrophy assessed by magnetic resonance imaging (MRI) is a good AD-biomarker at MCI stage. They accentuate that whole brain and hippocampus (HC) markers are too imprecise to identify people with increased risk of AD. A meta-analysis by Schmand, Huizenga & van Gool (2010) also indicates that MTL atrophy on MRI is currently not sensitive enough and does not offer diagnostic advantages over clinical symptoms in preclinical AD-phases.

Although there are encouraging findings supporting the idea, that even at MCI stage (Petersen et al., 2001) MTL atrophy predicts future AD fairly accurately (Mosconi et al., 2007; Twamley, Ropacki & Bondi, 2006), finding biomarkers reliably detecting the subtle pathological changes before further downstream clinical symptoms appear remains an important research goal. Assuming disease processes can already be detected in preclinical phases, structural MRI as an interface between the molecular pathology of AD and the clinical development occupies an important position (Frisoni et al., 2010). Optimising MRI-based biomarkers could have a significant impact on detecting and predicting AD-patients. Although currently no treatments completely halt the disease, studies underscore the need of diagnosis at prodromal stage when the pathologic injury is not severe (Lawrence, Pickett, Ballard & Murray, 2014).

MCI and parahippocampal atrophy

MCI due to AD forms the symptomatic predementia phase of AD and encompasses the transition-phase between healthy aging and dementia (Albert et al., 2013). Subjects with MCI show memory impairment beyond that expected for age and education (Petersen et al., 1999). Clinical criteria require impairment in one or more cognitive domains, but not severe enough for a diagnosis of dementia (Albert et al., 2013).

In the context of AD, the neurodegenerative pathology in MCI has been investigated in numerous studies. It was shown that cortical areas which form the PHG are susceptible to destructive processes of AD. In accordance with Braak and Braak (1991) studies showed that EC and PRC are the first to be damaged (van Hoesen, Augustinack, Dierking, Redman & Thangavel, 2000). Volumetric studies by Pantel et al. (2002) revealed that people with MCI only showed parahippocampal atrophy compared to older people who are cognitively normal (CN), suggesting that MCI individuals rank between CN and AD regarding their PHG integrity. Further imaging studies confirmed that people with MCI lie between CN individuals and AD-patients in terms of parahippocampal volume (Echávarri et al., 2011; Visser et al., 1999). People with AD have a reduced volume of the PHG compared to CN (Köhler et al., 1998; Kesslak, Nalcioglu & Cotman, 1991; Visser et al., 1999) and the PHG also allows a differentiation of CN vs. MCI (Devanand et al., 2012) even in early MCI stages (Chao et al., 2010). Especially in early MCI, the parahippocampal volume seems superior to hippocampal volume in differentiating CN, MCI, and AD (Echávarri et al., 2011). The EC in particular seems to predict future conversion from MCI to AD (de Toledo-Morrell, Goncharova, Dickerson, Wilson & Bennett, 2000; Devanand et al., 2012; Killiany et al., 2000), with the entorhinal volume also appearing superior to hippocampal volume (Dickerson et al., 2001).

Overall, investigating parahippocampal integrity is encouraging: It seems to allow a cross-sectional-based differentiation of the clinical stages CN, MCI and AD and might identify people with increased risk of developing severe impairments due to AD in early stages.

Parahippocampal variability limits its usefulness as AD-biomarker

As shown in Figure 1, the PHG is a bilateral structure of the MTL and lies inferior to Amygdala (AG) and HC (Raslau et al., 2015). It consists of distinct cortical structures. The EC is embedded medially in the PRC (Augustinack, van der Kouwe & Fischl, 2013), so these two cortices form the anterior region, whereas the parahippocampal cortex (PHC) forms the posterior portion of the PHG.

Even without AD, the PHG appearance can vary significantly between individuals. Firstly, parahippocampal volumes depend on psychological influencing factors (Meda et al., 2018; Zhou et al., 2016) and processes related to healthy aging (Sele, Liem, Mérillat & Jäncke, 2021).

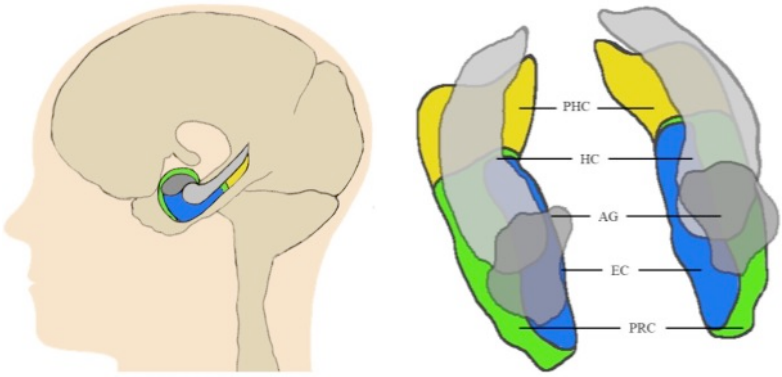

Figure 1. Parahippocampal anatomy. The PHG is a bilateral structure of the MTL and lies inferiorly to the AG (dark-grey) and the HC (light-grey). It consists of the EC (blue) and PRC (green) which form the medial and lateral parts of the anterior portion of the PHG, while the PHC (yellow) forms the posterior portion. Adapted from Raslau et al., 2015. PHG=parahippocampal gyrus; HC=hippocampus; AG=amygdala; PRC=perirhinal cortex; EC=entorhinal cortex; PHC=parahippocampal cortex.

Secondly, its characteristics are primarily determined by the shape of the collateral sulcus (CS) which runs along and is embedded in the PHG and can show substantial variations in length, depth and number of branches (Pruessner et al., 2002). In conclusion there is a high degree of variability in its appearance and volumetric properties between individuals.

As interindividual variability in brain anatomy limits the detection of AD using volumetric approaches (Coupé et al., 2012), the dependence of the PHG volume on the variability of the CS reduces the usefulness for early AD-diagnosis. It must be assumed that the absolute parahippocampal volume is not sufficiently valid, sensitive, and reliable. In short: a small PHG does not necessarily indicate a loss of its integrity.

Presenting a relative measure for parahippocampal integrity: CSR

In summary, due to its early involvement, parahippocampal volume seems to be good in estimating the development of AD. However, the promising diagnostic utility is limited by the variability of its anatomy. An optimised MRI-based biomarker that accounts for this variability could be beneficial.

Schoemaker and colleagues (2019) showed that, compared to the absolute HC volume, the Hippocampal-to-Ventricle-Ratio generated by associating volumes from HC and its surrounding ventricles is a reliable measurement for hippocampal integrity. By relating cortical volumes of PHG and the volume of the CS the generated parahippocampal Cortex-to-Sulcus-Ratio (CSR) transfers the idea of a relative integrity measure to the PHG. The basic assumption behind CSR is that there is a certain space for parahippocampal cortices and the CS that remains unchanged even if the volumetric ratio of cortex and sulcus shifts. With maximum expression of parahippocampal cortices in a CN stage, the sulcal volume is minimal. Parahippocampal atrophy as a result of AD neuropathology is believed to be associated with increasing sulcal widening (Im et al., 2008). Relating cortex and sulcus is thought of correcting the parahippocampal volume for the CS variability and to overcome the effects of anatomical variability in general population. In fact, it has been shown that taking into account the CS reduces the within-group variance when assessing para-hippocampal integrity (Pruessner et al., 2002).

The aim is to validate the CSR as measure of parahippocampal integrity cross-sectionally estimating the AD-status. It is assumed that this relative measurement corrects normally occurring variations in the absolute parahippocampal volume and allows an improved differentiation between changes in parahippocampal volume associated with normal or pathological aging. From a clinical perspective the hypothesis is that compared to the standard absolute parahippocampal volume the CSR allows a clearer distinction between older adults being CN, MCI, or AD. More abstractly, it is hypothesised there are substantial differences among the absolute and relative integrity measurements between groups, so that in a two-factorial comparison a significant interaction effect can be observed. The hypothesis is illustrated in Figure 2.

With the goal of finding a biomarker detecting AD early these assumptions were tested in an MRI-study. The procedure is based on the aim of assessing the ability to distinguish individuals with and without AD (Frisoni et al., 2017). Absolute volumetric measurements and the CSR were compared in a sample of older adults categorised as either CN, MCI, or AD.

To examine which parahippocampal structures might be particularly relevant, volumes of the manually segmented cortices are considered in combination and individually.

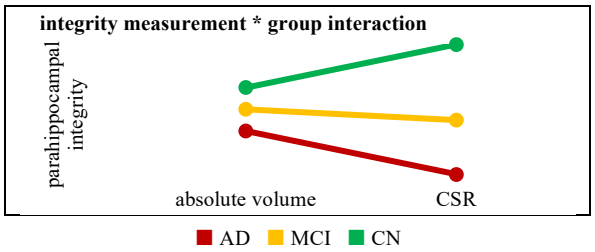

Figure 2. Visualised main hypothesis of a (semi-) disordinal interaction of the factors Integrity measurement*Group. Assuming a uniform scale level, the two levels of the factor Integrity measurement are presented on the x-axis. Levels of the factor Group were used to create separate lines. CSR=Cortex-to-Sulcus-Ratio; AD=Alzheimer's disease; MCI=mild cognitive impairment; CN=cognitively normal.

Methods and Material

Participants and procedures

Study sample. The current study is based on the third release of the Open Access Series of Imaging Studies (OASIS-3; LaMontagne et al., 2019) which focusses on the effects of healthy aging and AD. The data set contains various information on a total of 1098 older adults who were consented into projects following procedures approved by the Institutional Review Board of the Washington University School of Medicine. The multimodal data are freely available to the scientific community at https://www.oasis-brains.org.

Clinical and cognitive assessments of OASIS-3 are standardised through the National Alzheimer's Coordinating Center Uniform Data Set (Beekly et al., 2007; Morris et al., 2006) which includes clinical and cognitive assessment. Dementia status was evaluated using the Washington University Clinical Dementia Rating (CDR) which provides a standardised assessment of cognitive functioning through assessments of memory, orientation, judgment and problem solving, community affairs, home and hobbies, and personal care (Morris, 1993, 1997).

For cross-sectional group comparisons according to the current study aim, based on their CDR diagnosis eight subjects each from the following groups were included in the present study: CN, MCI and AD. Overall cross-sectional scans from a total sample size of N=24 people aged between 58 and 80 years were examined. Additional demographic characteristics such as gender or level of education are not available and were not considered in the analysis, according to Frisoni et al. (2017) this is a secondary goal of subsequent research phases.

Exclusion criteria for OASIS-3 (LaMontagne et al., 2019) were medical contraindications for study participation such as claustrophobia or implanted medical devices like pacemaker and drug pump for MRI. Eligible participants signed informed consent and agreed to the use of their data by the scientific community.

MRI Acquisition. Neuroimaging scans were obtained from the Knight Alzheimer Research Imaging Program at Washington University in St. Louis (LaMontagne et al., 2019). MRI was acquired using three different Siemens scanner models (Siemens Medical Solutions USA, Inc): Vision 1.5T, TIM Trio 3T (2 different scanners of this model) and BioGraph mMR PET-MR 3T. Subjects were placed in a 16-channel head coil on 1.5T scanners and 20-channel head coil on 3T scanners using foam pad stabilizers placed next to the ears to reduce movement. For the purpose of the present work only the T1-weighted images with a slice spacing of 1 mm were used.

MRI Analyses

Preprocessing. Raw OASIS-3 images were downloaded in NifTI format and transformed to MNC format, which is fitted to the MINC toolkit. To prepare the T1-weighted images for manual segmentation, first of all they were denoised (Coupe et al., 2008) and subsequently corrected for intensity non-uniformity (Sled, Zijdenbos & Evans, 1998). To control for brain size and shape differences, the images were registered to the Montreal Neurological Institute Standard Space template (MNI 152; Collins, Neelin, Peters & Evans, 1994). Finally, to ensure the quality of the preprocessing a visual inspection of the images was performed.

Volumetric segmentation of the PHG. During volumetric segmentation of the PHG, the participants group affiliation was unknown. Volumetric analyses were performed using the open-source software DISPLAY, which is part of the MINC toolkit package developed at the Montreal Neurological Institute's Brain Imaging Center (https://bic-mni.github.io/). This interactive software package allows the brain images to be inspected simultaneously in coronal, sagittal, and

horizontal orientation, resulting in contiguous 1 mm slices for 3D navigation through the brain at 1 mm intervals. Any desired viewing angle can also be set in an additional fourth window, so the target structure can be viewed from any required perspective. For improved visualisation of the MTL (de Leon et al., 1997), a perspective along the anterior commissure - posterior commissure line and the line perpendicular to the long axis of the HC was chosen for the additional window, so that the image is aligned parallel to the CS. The program allows for segmentation in all perspectives, labelled structures in the three standard orientations appear immediately in all orientations shown.

The anatomical boundaries to determine the parahippocampal volumes and generate the CSR were obtained from the protocol for manual segmentation of the PHG by Pruessner et al. (2002) which is directly derived from the histopathological studies by Insausti et al. (1998) and represents a reliable segmentation protocol. Since the current study is largely based on the segmentation of the PHG, the guidelines used to label PRC, EC and PHC and particularly modifications compared to Pruessner et al. (2002) are described in detail below. Figure 3 shows the segmentation of the PHG graphically. Coronary sections of the left PHG were intended to illustrate different volumetric relationships of the cortical structures to the adjacent sulcus. For this purpose, images of CN subjects with a small CS are depicted on the left (Figure 3A, C) and images of AD-subjects with a noticeably enlarged CS on the right (Figure 3B, D).

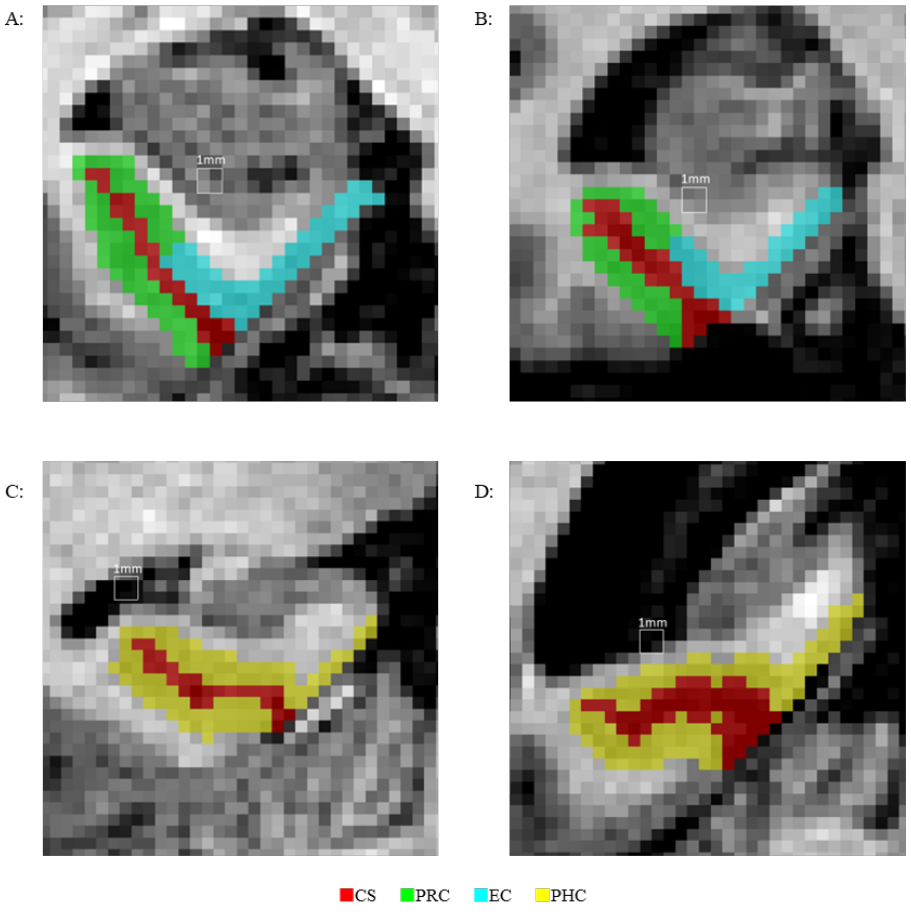

Figure 3. Segmentation of the PHG. Coronal slices of the left PHG were chosen to illustrate volumetric proportions of cortex and CS for CN subjects on the left and AD patients on the right. The upper row shows the segmentation of the PRC and EC in CN (A) and AD (B) subjects. Segmentation of the PHC In CN (C) and AD (D) subjects is depicted below. PHG=parahippocampal gyrus; CS=collateral sulcus; PRC=perirhinal cortex; EC=entorhinal cortex; PHC=parahippocampal cortex; CN=cognitively normal; AD=Alzheimer's disease.

Before the actual segmentation of the PHG important landmarks in the brain were identified that determined important characteristics of the PHG and the transitions of the individual cortices. Determining

these landmarks requires knowledge of the protocol for segmentation of HC and AG by Pruessner et al. (2000).

The anterior end of the AG defines the anterior end of the PRC and EC. The most posterior HC slice in the coronal view was chosen as the posterior end of the PHC and thus the PHG. A final important landmark marking the transition from EC to PRC to PHC was the disappearance of the gyrus intralimbicus (GIL). This gyrus lies approximately midway in the rostrocaudal extension from AG to HC and can be easily identified in the sagittal view. An exact localisation can then be made in the coronal view.

The segmentation of the CS and the cortical structures of the PHG was mainly performed at the coronal plane, with other perspectives used whenever they gave supplementary information. Before the cortices were labelled, a lot of emphasis was placed on the careful segmentation of the CS. The cortices were segmented from rostral to caudal direction, so the grey matter of the PRC and EC was labelled before the PHC. Overall, the grey matter surrounding the CS representing the respective cortex, could usually be delimited from white matter superiorly and laterally. Inferiomedially, cerebrospinal fluid and dura defined the border of the cortices. The presence of dura could be verified primarily in a horizontal view. The dura itself was excluded from labelling. The target structures were only labelled if they could clearly be identified. To account for this modification compared to Pruessner et al. (2002), finally the number of labelled coronary slices of the respective cortices was determined for each subject.

CS. Since the sulcal volume plays a central role in this work and the localisation of the relevant cortical structures in the PHG depends largely on the appearance of the CS, great vigilance was attached to its reliable identification and delimitation. For this purpose, a coronal section in the posterior part of the HC was initially selected, in which the CS was clearly visible from the fundus to the cortical surface, i.e., without a side branch to an adjacent sulcus of the MTL or an interruption. When the CS could be reliably identified, it was labelled as such from the fundus to its cortical surface or the medial dura. On the one hand, the depth had to be at least 4 mm or 2.5 diagonal voxels, and on the other hand, the sulcus had to be surrounded by a (semi)circle of grey matter, which formed the surrounding PHG. To meet the goal of this work, the CS was not consistently labelled with a width of 1 voxel, as Pruessner et al. (2002) did, but instead its actual appearance was considered. Since the rostro-caudal extent of the target-relevant cortical structures was defined by specific landmarks, an exact determination of the anterior and posterior borders of the CS was not necessary. To validate and refine the segmentation, all perspectives, especially the additional window, were regarded. Ultimately, the depth of the CS was labelled on each coronary slice from the anterior end of the AG to the most posterior HC slice. In the event of an interruption, the occurrence of a side branch of the CS or the connection to the adjacent occipitotemporal sulcus (OTS), additional perspectives were taken for validation and segmentation, with the additional window aligned parallel to the CS being particularly helpful in these cases. The following additional rules were formulated to ensure uniform labelling for these irregularities as well: When a connection of CS and OTS occurred, it had to be decided to what extent the connecting sulcus was to be regarded as a side branch of the CS. Firstly, this side branch was allowed to be no more than 10 mm from the main sulcus, and secondly, the side branch had to appear together with the main sulcus. The side branch was only labelled as such if it met both conditions. In contrast to Pruessner et al. (2002), no extrapolation was carried out in the case of an interruption of the CS or the cortex in the coronal perspective. Instead, a correction based on the number of labelled slices was later performed.

PRC. Against the segmentation protocol of Pruessner et al. (2002), the anterior end of the PRC was defined via the most anterior coronary AG slice which determines the rostral extent of the PHG according to the labelling approach used. In the caudal direction, the PRC extends in accordance with the segmentation rules of Pruessner and colleagues (2002) depending on the GIL: the last coronary slice labelled as PRC lies 4 mm posterior to the disappearance of the GIL. On the two most anterior and most posterior coronary PRC slices, the gyrus surrounding the CS was exclusively labelled as PRC, whereas in the area between the EC is embedded medially in the PRC (Figure 3A, B). To delineate PRC and EC, where the EC is embedded medially into the PRC, the inferomedial PRC border was chosen independently of the depth of the sulcus at the medial midpoint of the most medial CS. In the two most anterior and most posterior coronary exclusive PRC slices, respectively, the superolateral portions of the PRC approached the inferomedial border of AG and HC, respectively. There was usually no direct connection between the PRC and the structures located superiorlaterally. The structures were either delimited by a band of white

matter or further anterior by the presence of the sulcus semianularis. If neither was evident, an imaginary white matter extension line was drawn to differentiate the structures, excluding one row of grey matter voxels to account for the partial volume effect. The inferolateral demarcation from the occipitotemporal cortex (OTC) depends on the appearance of the CS but follows uniform rules over the entire rostrocaudal extent of the PRC. If there was only one CS, the PRC was labelled up to the lateral bank of the CS. If there were multiple CS, labelling was performed up to the fundus of the most lateral CS.

EC. The rostrcaudal extension of the EC depends on the PRC. The anterior border was defined 2 mm posterior to the most anterior coronary AG slice. Caudally, the EC terminates 2 mm posterior to the disappearance of the GIL and is then replaced by the PRC for a further 2 mm. Just like the PRC, further anterior the EC lies inferior to the AG and further posterior it lies inferior to the HC. The demarcation of the EC from these superior structures is equivalent to the PRC. The EC is embedded medially into the PRC and laterally borders to the CS. The superolateral boundary to the PRC was defined via the midpoint of the most medial CS, regardless of the depth of the sulcus.

PHC. On the coronary slice 5 mm posterior to the disappearance of the GIL, the PHC replaces the PRC and thus forms the anterior PHC border. Caudally, the PHC extends to the posterior end of the HC. Equivalent to the delimitation of PRC and OTC, the inferolateral boundary of the PHC was also defined by the cortical surface at its lateral bank in the case of one CS (Figure 3C, D) or by the fundus of the most lateral CS in the case of multiple CS. The demarcation of the PHC from structures lying superiorly follows the segmentation rule of the superolateral border of the PRC when no EC is present. If the calcarine sulcus was present more posteriorly, its inferior border formed the superior border of the PHC.

Absolute and relative measurement of parahippocampal integrity: Absolute volume vs. CSR

The volumes of the manually labelled structures were calculated automatically by the software. Since, unlike Pruessner et al. (2002), sulcus and cortices were not labelled continuously, but only when they could clearly be identified, the generated volumes were corrected based on the number of labelled slices. For the standard absolute measurement of parahippocampal integrity, this means that it is operationalised by the quotient of the respective total volume of a specific structure by the number of labelled slices – resulting in a slicewise volume referred to as absolute volume in the following. According to the number of labelled cortices and corresponding sulcus sections per hemisphere, eight values of this absolute volume for cortex and sulcus were determined for each subject. Per hemisphere there was a value for the PRC, EC, PHC and a total measure of the PHG and the corresponding sulcus sections.

Analogous to the Hippocampal-to-Ventricle-Ratio (Schoemaker et al., 2019), generating a relative measurement of parahippocampal integrity is based on the assumption that the widening of the sulcus embedded in the PHG as a result of cortical atrophy can be represented as a function of the neurodegeneration of the parahippocampal cortices. Thus, with increasing atrophy, an increasing sulcal expansion can be observed. Calculating a ratio that reflects the relationship between the absolute cortex and sulcus volumes is thought of providing a relative measurement of the integrity of the respective cortical target structures of the PHG. The following formula was derived to calculate the Cortex-to-Sulcus-Ratio (CSR):

$$\frac{absolute\ cortical\ volume}{absolute\ cortical\ volume\ +absolute\ volume\ of\ adjecent\ sulcus}$$

Based on the idea that the sulcal section adjacent to the affected cortical structure expands as a result of cortical neurodegeneration or loss of integrity, in this formula the absolute volume of the respective cortical structure is divided by the sum of the absolute volumes of the respective cortex structure plus the adjacent sulcus section.

The interpretation of the ratio is illustrated by examining a very small versus a very large sulcus volume: In the case of a very small sulcus (close to volume 0), the CSR is large, at most 1, because the cortical volume is almost divided by itself. This can be imagined as an ideal case with almost no neurodegeneration in the PHG or no sulcal widening. With a very large CS, the CSR will be significantly smaller than 1 since the sulcal expansion now has a greater impact on the integrity index. With an index value of 0.5, one could assume that the cortex and sulcus take up the same proportion of volume in the available space. The closer the CSR is to 0, the greater the (hypothetical) cortical atrophy or sulcus widening.

Transformation

Since a comparison of the actual values operationalising the absolute and relative measurement of

parahippocampal integrity is not helpful due to the different scaling of the absolute volume and the CSR, integrity values of all cortices were z-standardised across the whole group prior the statistical analyses. This type of transformation preserves the relative position of the values and thus the original form of distribution.

Interpreting the z-transformed parameters and the results of the analyses, however, it must be taken into account that one is not actually dealing with the integrity measures in the sense of the absolute cortical volumes or the CSR. Instead, considering groupwise means of these z-standardised variables enables the groups to be classified into the overall distribution of the values of the respective variable across all groups. For example, a group mean of 1 for a designated integrity measurement of a particular cortex would mean that this group is on average one standard deviation above the overall mean for the specific cortical integrity. A positive group mean means that the parahippocampal integrity of this group is above the average for the total sample, as it would be assumed for the CN group. Whereas a below-average cortical integrity would be characterised by a negative group mean and is expected for individuals with AD. In terms of cortical integrity, people with MCI are assumed to be some-where between AD and CN. In the case of the z-transformed variable the groupwise standard deviation represents the relation of the non-transformed groupwise standard deviation and the non-transformed standard deviation across all groups and it can be interpreted as a measure of dispersion around the central tendency of the group's integrity values. The average values of the z-transformed measurements of parahippocampal integrity per group are presented in Table 1.

According to the hypothesis, that the differentiating the parahippocampal integrity of the groups is improved if in addition to the cortical volume of the PHG the volume of the adjacent CS is considered, it is expected that the groupwise means of the z-standardised integrity measures for the particular cortex lie closer together for the absolute integrity measure than for the relative one. Looking at the absolute volume is thought of not necessarily allowing a clear distinction of the clinical conditions. Whereas following the postulated superiority of the relative integrity measure it is assumed that the z-standardised groupwise means of the CSR drift apart, i.e., within groups they take on more mutually similar and extreme values compared to the overall distribution, so that a clearer differentiation of the groups is possible.

Deriving the statistical method

The study follows a 2*3 split plot design. The measurement of parahippocampal integrity represents the within factor. By determining the absolute, operationalised by the absolute cortical volumes, and relative, operationalised by the CSR, measures for each cortex, each subject provides values for the two levels of the within factor. The group forms the between factor: the CDR-Score categorises each subject as either AD, MCI or CN.

Taking into account the study design the statistical analyses examining whether substantial differences occur among the levels of integrity between the groups, should follow a two-factorial design with repeated measurements on one factor. As Sele et al. (2021) demonstrated that healthy aging subjects show a significant decrease in parahippocampal volume with increasing age, it is assumed that independent of the clinical condition the absolute cortical volumes and the CSR which operationalise the parahippocampal integrity measurements are also determined by a linear dependence with age. The linear relationship of the integrity measurements and age was checked visually in scatterplots. Separated by parahippocampal structure, hemisphere and integrity measurement these scatterplots are presented in Figure A.1 and A.2 in the Appendix. Additionally, one-tailed bivariate analyses were computed to measure the strength of the negative association be-tween the two variables. To reduce the influence of age on the parahippocampal integrity in the statistical analyses, this variable was considered as a covariate (Federer & Meridith, 1992).

Mixed model analyses of covariance (ANCOVA) with the within-subjects factor parahippocampal integrity measurement and the between-subjects factor group were conducted to determine whether significant differences exist among the absolute and relative cortical integrity measure between the levels of the groups (hypothesised interaction effects) after controlling for the participant's age. According to the number of cortical structures tested per hemisphere, a total of eight analyses were performed.

Table 1
Summary of z-transformed and age adjusted values M(SD) for the absolute and relative measurement of parahippocampal integrity separated by cortical structures and hemisphere

		Left PHG (*N*=23)		**Right PHG** (*N*=22)	
		Absolute [b]	CSR [c]	Absolute [b]	CSR [c]
z-transformed	AD	-.90 (0.83)	-.55 (0.76)	-.19 (1.04)	-.45 (1.11)
	MCI	.72(0.79)	-.21 (1.23)	.02 (1.23)	-.27 (0.79)
	CN	.27 (0.62)	.73 (0.51)	.20 (0.78)	.78 (0.61)
age-adjusted [a]	AD	-.73 (0.23)	-.57 (0.32)	.19 (0.30)	-.31 (0.32)
	MCI	.75 (0.24)	-.21 (0.34)	.15 (0.30)	-.22 (0.33)
	CN	.08 (0.24)	.75 (0.33)	-.36 (0.33)	.58 (0.36)

		Left PRC (*N*=23)		**Right PRC** (*N*=23)	
		Absolute [b]	CSR [c]	Absolute [b]	CSR [c]
z-transformed	AD	-.75 (0.79)	-.50 (0.83)	-.02 (0.88)	-.50 (1.23)
	MCI	.73 (0.78)	-.33 (1.08)	.11 (1.45)	-.01 (0.72)
	CN	.11 (0.90)	.79 (0.60)	-.08 (0.75)	.51 (0.78)
age-adjusted [a]	AD	-.63 (0.29)	-.53 (0.32)	.20 (0.34)	-.44 (0.35)
	MCI	.75 (0.30)	-.34 (0.33)	.15 (0.35)	-.01 (0.36)
	CN	-.03 (0.29)	.83 (0.32)	-.34 (0.34)	.45 (0.35)

		Left EC (*N*=23)		**Right EC** (*N*=22)	
		Absolute [b]	CSR [c]	Absolute [b]	CSR [c]
z-transformed	AD	-.63 (1.03)	-.35 (0.97)	-.04 (1.41)	-.42 (1.02)
	MCI	.49 (1.02)	-.31 (1.10)	-.22 (1.00)	-.14 (0.88)
	CN	.20 (0.67)	.62 (0.70)	.27 (0.22)	.62 (0.91)
age-adjusted [a]	AD	-.43 (0.29)	-.33 (0.35)	.13 (0.33)	-.42 (0.35)
	MCI	.53 (0.30)	-.30 (0.36)	-.21 (0.35)	-.14 (0.37)
	CN	-.04 (0.29)	.59 (0.35)	-.06 (0.36)	.62 (0.38)

		Left PHC (*N*=23)		**Right PHC** (*N*=23)	
		Absolute [b]	CSR [c]	Absolute [b]	CSR [c]
z-transformed	AD	-.57 (0.89)	-.72 (0.68)	-.34 (1.03)	-.15 (0.85)
	MCI	.37 (0.70)	.07 (1.07)	.12 (1.14)	-.62 (0.98)
	CN	.24 (1.16)	.66 (0.78)	.24 (0.87)	.69 (0.80)
age-adjusted [a]	AD	-.51 (0.35)	-.73 (0.32)	-.16 (0.34)	-.06 (0.32)
	MCI	.38 (0.37)	.07 (0.33)	.16 (0.35)	-.60 (0.33)
	CN	.18 (0.36)	.67 (0.32)	.02 (0.34)	.60 (0.32)

Notes. [a] covariate-adjusted means were calculated using the grand mean of the covariate (age=69.04 for *N*=23; age=68.55 for PHG right; age=69.45 for EC right). [b] absolute integrity measure uses absolute cortical volume. [c] relative integrity measure uses CSR. CSR=Cortex-to-Sulcus-Ratio; PHG=total parahippocampal gyrus; PRC=perirhinal cortex; EC=entorhinal cortex; PHC=parahippocampal cortex; AD=Alzheimer's disease; MCI=mild cognitive impairment; CN=cognitively normal.

Results

All analyses were performed using Microsoft Excel and IBM SPSS Statistics for Windows (Version 29). A significance level of 5% was set for the statistical tests.

Data Cleansing

Due to poor image quality, one subject from the MCI group had to be excluded from the analysis, as there was no volumetric data available. The further identification of outliers is based on the integrity data of the different cortical structures, so that group-wise

boxplots were formed for all dependent variables. Extreme outliers were identified by visual inspection of the boxplots. Subjects were excluded from the analyses for each cortical structure if their datapoints were placed at least three times the interquartile range away from the first or third quartile. With an above-average value for the absolute volume of the right EC, one person had to be excluded from the CN group for the analyses of the right EC according to this rule.

Sample Characteristics and Descriptive Data

The mean age for CN subjects was 66 years, for MCI subjects 69.57 years and for AD-patients 71.63 years. To check whether the participants age varies systematically with the group a one-way analysis of variance (ANOVA) was conducted. The main effect for group did not reach significance, $F(2, 20)=1.57$, $p=.232$. Subjects' age was consistently negatively associated with parahippocampal integrity, with Pearson's correlation coefficients, presented in Figure A.1 and A.2 in the Appendix, suggesting stronger associations between age and absolute cortical volume than age and CSR values. Since there is no information on gender and level of education, no further statements can be made about sample characteristics.

Minimum and maximum volumes of the parahippocampal structures, means and standard deviations are presented in Table A in the Appendix, separately for left and right hemisphere. According to the different types of integrity measurements, both the uncorrected and absolute (slicewise) volumes of the individual cortical structures and adjacent sulci as well as the CSR are presented across all groups and individually for the respective sample of NC, MCI and AD.

A comparison of the mean values of the CN participants uncorrected cortical volumes with those reported by Pruessner et al. (2002) revealed considerable differences in the assessment of all segmented structures. The absolute uncorrected volumes are consistently lower for all investigated cortical structures in this study (PRC left 2502 mm3 in Pruessner vs. 1220 mm3 in this study; PRC right 2417 mm3 in Pruessner vs. 1121 mm3 in this study; EC left 1553 mm3 in Pruessner vs. 853 mm3 in this study; EC right 1672 mm3 in Pruessner vs. 858 mm3 in this study; PHC left 2675 mm3 in Pruessner vs. 1804 mm3 in this study; PHC right 2469 mm3 in Pruessner vs. 1782 mm3 in this study). However, in this comparison it must be borne in mind that although the current segmentation was based on the protocol of Pruessner et al. (2002), some important segmentation guidelines were modified and adapted to the aim of this work. For example, the CS was not consistently labelled with a width of 1 voxel, and slices on which the sulcus and/or cortex were not recognisable were omitted. To correct for this exclusion in the analysis, the uncorrected volume divided by the number of labelled slices was chosen as the dependent variable. Furthermore, as age is a factor influencing parahippocampal volume (Sele et al., 2021), the different volumes could be partly explained by the different age of the study sample. Subjects in the study of Pruessner et al. (2002) were in early adulthood, between 18 and 42 years of age which does not match with the CN group ranging from 60 to 80 years investigated in the present study. Since a description of the interaction effects in the context of the ANCOVA results will go into more detail later, no further description of the calculated values for the absolute and relative integrity measurements is given at this point.

Assumptions

Before running the analyses, the methods assumptions were assessed using the respective pertinent variables. Mixed ANCOVAs including customised interaction terms of group and age were conducted to assess the homogeneity of regression slopes. If there are significant interactions between an independent variable and a covariate, the assumption is violated (Pituch & Stevens, 2016). Most of the interactions of interest did not reach significance ($p>.05$), indicating homogeneity of regression slopes in these cases. However, the relevant interaction terms did reach significance for the right PHG and the right EC, which means that in these cases the assumption was not met. Since the interactions are particularly meaningful in the current analyses, and these cannot be interpreted if this assumption is violated, group-wise boxplots for age were inspected to discover and correct for possible outliers. Therefore, one person from the CN group who was slightly above average age was excluded in the analyses of the right PHG. Homogeneity of the regression slopes could then be assumed for this variable. No correction could be made for the violation of the assumption for the right EC, which must be taken into account when interpreting the results.

The between-subjects factor and the covariate must be independent of each other (Miller & Chapman, 2001). As mentioned above, a non-significant one-way ANOVA revealed, that the participants age does not vary systematically with the group indicating that the assumption was met.

To check the normal distribution of the residuals in the groups Q-Q scatterplots were visually inspected. In these plots a line represents the theoretical quantiles of a normal distribution and if the points form a relatively straight line normality can be assumed (Field, 2013). The scatterplots indicate normality for all variables.

Homoscedasticity was evaluated by running Levene's Tests, all of which did not reach significance (all $p>.05$), so that homoscedasticity can be assumed for all variables (Field, 2013).

The equality of the covariance matrices was evaluated using Box's M tests (Box, 1949). In almost all cases no significance was reached, so the assumption of homogenous covariance matrices can be considered to be met for all variables except the right EC ($p=.042$).

Since the within-factor has only two levels of repeated measurements, the sphericity assumption has not to be tested.

ANCOVA results

Prior to a more specific description of the important interaction effects the main effects of the between and within-factors are briefly illustrated. Due to the large number of analyses, only results that meet the significance level of 5% are reported below. The results of all statistical analyses are summarised in Table 2, separated by cortical structure and hemisphere.

The covariate age was significantly related to the absolute and relative integrity measure for the right total PHG with $F(1, 18)=11.54$, $p=.003$ and partial $\eta^2=.39$ and the right PRC with $F(1, 19)=6.5$, $p=.02$ and partial $\eta^2=.26$. The main effect for the between factor group reached significance for the total PHG left with $F(2, 19)=6.19$, $p=.008$ and partial $\eta^2=.40$, the left PRC with $F(2, 19)=7.86$, $p=.003$ and partial $\eta^2=.45$ and the left PHC with $F(2, 19)=4.56$, $p=.024$ and partial $\eta^2=.32$. This indicates that for these cortical structures there were significant differences between groups, regardless of the integrity measurement, after controlling for age. The main effect for the within-subjects factor integrity was significant for the left PHG with $F(1, 19)=4.83$, $p=.041$ and partial $\eta^2=.2$ and the left EC with $F(1, 19)=4.39$, $p=.05$ and partial $\eta^2=.19$, indicating that in these cases were significant differences between the absolute and relative integrity measurements, regardless of the group, after controlling for age.

The covariate-adjusted means were calculated using the grand mean value of the covariate and are presented in Table 1. To compare the age-adjusted means, the Figures 4.1 to 4.8 show interaction plots separated by parahippocampal structure and hemisphere. In these plots each point represents a z-transformed, age-adjusted group mean of the absolute or the relative integrity measure for the specific cortical structure. For a clearer differentiation of the groups regarding the overall distribution, a solid line with y=0 marks the overall mean. Levels of the between factor were used to create separate lines for the groups. Nonparallel lines indicate an interaction between factors.

Firstly, it can be seen that, according to the hypothesis, the relative integrity data points are actually drifting apart, i.e., the lines are not parallel, indicating interactions. The fact that in general the age-adjusted group means assume more extreme values for the CSR implies that for this relative integrity measure the groups values deviate more strongly from the overall mean, which also makes differentiation of these groups easier. On average, when the CSR is considered instead of the absolute volumes, CN individuals seem to have higher parahippocampal integrity scores. Especially MCI individuals, but also AD, showed considerably lower parahippocampal integrity when looking at the CSR.

Secondly, one recognises that with the relative integrity measurement, with the exception of the right PHC, the assumed order of the group mean values is maintained, whereas this is not the case for the absolute integrity measurement. This indicates disordinal interactions. With a range of age-adjusted group means from 0.45 to 0.83, the relative integrity of individuals of the CN group averages 0.64 standard deviations and consistently above the overall sample mean when the CSR is used to assess parahippocampal integrity. As expected, the transformed and adjusted CSR group means of all cortical structures are negative for AD and range from -0.73 to -0.06. On average, the group-wise relative parahippocampal integrity is 0.42 times standard deviation below the mean of the overall sample. The assumption that people with AD have the lowest mean relative parahippocampal integrity is satisfied for all cortical structures except for the right PHC. On average, people with MCI showed even lower relative integrity values for this structure. Aside from that, as assumed, people with MCI were on average between people with AD and CN in terms of the relative cortical integrity.

Table 2. ANCOVA results for the cortical structures separated by hemisphere

	Left PHG (*N*=23)						**Right PHG** (*N*=22)					
Source	*df*	*SS*	*MS*	*F*	*p*	η^2	*df*	*SS*	*MS*	*F*	*p*	η^2
Between												
Age	1	1.48	1.48	1.94	.179	.09	1	8.49	8.49	11.54	**.003**	.39
Group	2	9.46	4.73	6.19	**.008**	.40	2	.18	.09	.12	.886	.01
Residuals	19	14.51	.76				18	13.25	.74			
Within												
Integrity	1	2.07	2.07	4.83	**.041**	.20	1	1.83	1.83	2.89	.106	.14
I*A	1	2.06	2.06	4.79	**.041**	.20	1	1.85	1.85	2.92	.105	.14
I*G	2	5.05	2.52	5.88	**.010**	.38	2	3.38	1.69	2.67	.097	.23
Residuals	19	8.16	.43				18	11.41	.64			

	Left PRC (*N*=23)						**Right PRC** (*N*=23)					
Source	*df*	*SS*	*MS*	*F*	*p*	η^2	*df*	*SS*	*MS*	*F*	*p*	η^2
Between												
Age	1	.49	.49	1.01	.327	.05	1	4.65	4.65	6.50	**.020**	.26
Group	2	7.61	3.80	7.86	**.003**	.45	2	.34	.17	.24	.791	.02
Residuals	19	9.19	.48				19	13.59	.72			
Within												
Integrity	1	1.54	1.54	1.74	.203	.08	1	1.50	1.50	1.43	.247	.07
I*A	1	1.52	1.52	1.72	.206	.08	1	1.51	1.51	1.44	.246	.07
I*G	2	6.86	3.43	3.88	**.039**	.29	2	3.61	1.80	1.71	.207	.15
Residuals	19	16.78	.88				19	19.98	1.05			

	Left EC (*N*=23)						**Right EC** (*N*=22)					
Source	*df*	*SS*	*MS*	*F*	*p*	η^2	*df*	*SS*	*MS*	*F*	*p*	η^2
Between												
Age	1	3.34	3.34	3.05	.097	.14	1	2.33	2.33	2.41	.138	.12
Group	2	3.23	1.62	1.48	.253	.14	2	2.23	1.11	1.15	.338	.11
Residuals	19	20.76	1.09				18	17.38	.97			
Within												
Integrity	1	1.88	1.88	4.39	**.050**	.19	1	2.56	2.56	3.14	.093	.15
I*A	1	1.86	1.86	4.36	.051	.19	1	2.60	2.60	3.19	.091	.15
I*G	2	3.88	1.94	4.54	**.025**	.32	2	2.11	1.05	1.29	.298	.13
Residuals	19	8.13	.43				18	14.66	.81			

	Left PHC (*N*=23)						**Right PHC** (*N*=23)					
Source	*df*	*SS*	*MS*	*F*	*p*	η^2	*df*	*SS*	*MS*	*F*	*p*	η^2
Between												
Age	1	.12	.12	.13	.723	.01	1	4.52	4.52	4.02	.059	.18
Group	2	8.68	4.34	4.56	**.024**	.32	2	2.16	1.08	.96	.401	.09
Residuals	19	18.08	.95				19	21.38	1.13			
Within												
Integrity	1	.25	.35	.35	.563	.02	1	.56	.56	1.15	.298	.06
I*A	1	.25	.25	.34	.564	.02	1	.55	.55	1.13	.302	.06
I*G	2	1.36	.68	.93	.414	.09	2	3.24	1.17	3.29	.059	.26
Residuals	19	13.91	.73				19	9.34	.49			

Notes. Significant effects are indicated by bold p-values. PHG=total parahippocampal gyrus; PRC=perirhinal cortex; EC=entorhinal cortex; PHC=parahippocampal cortex; I*A=Interaction Integrity*Age; I*G=Interaction Integrity*Group.

With the exception of the left PHC (0.07), the age-adjusted group means are consistently negative and, with a range of -0.6 to -0.01, lie on average 0.22 standard deviations below the relative parahippocampal integrity of the overall mean.

Although the situation described seems to be very remarkable, the large variance in the data must also be taken into account. For a statistical validation of this situation described above the interaction effects of the within-subjects factor and the between-subjects factor are considered in the following. On the one hand, the significance of the integrity*group-interactions could be confirmed for two cortical structures on the left hemisphere. The interaction for the left PRC, $F(2, 19)=3.88$, $p=.039$ and partial $\eta^2=.29$, as well as the left EC, $F(2, 19)=4.54$, $p=.025$ and partial $\eta^2=.32$, reached significance. Along with that also the interaction for the left total PHG was significant with $F(2, 19)=5.88$, $p=.01$ and partial $\eta^2=.38$. On the other hand, for the right hemisphere there was no integrity*group-interaction that reached significance at a 5% level. However, the relevant interaction for the right PHC was marginally significant with $F(2, 19)=3.29$, $p=.059$ and partial $\eta^2=.26$. But considering this interaction, it must be taken into account that, as mentioned above, the adjusted CSR group means for this cortical structure did not follow the expected order. It should be noted that none of these significant interactions meets the statistical threshold of 5% when Bonferroni corrections were performed. According to Cohen (1988) all of the significant within-between interactions reached large effect sizes ($\eta^2>.14$).

Discussion

A novel ratio estimating the integrity of the parahippocampal gyrus (PHG) was introduced. It was based on the assumption that correcting for naturally occurring variations in the PHG improves differentiation between changes in the parahippocampal volume associated with healthy or pathological aging in terms of Alzheimer's disease (AD). By relating volumetric measurements of cortical structures and adjacent sulcal expression, the Cortex-to-Sulcus-Ratio (CSR) accounts for the collateral sulcus (CS) which highly determines the shape of the PHG. Refining the estimation of parahippocampal integrity, the aim of this work was to take a first step in validating a new, potentially useful biomarker for early detection of AD. The hypothesis, that the CSR is superior to the standardly used absolute parahippocampal volume in differentiating healthy aging individuals, people with mild cognitive impairment (MCI) and AD-patients, particularly when relying on cross-sectional data, was tested in a magnetic resonance imaging (MRI) study, comparing manually segmented brains.

Indeed, descriptive comparisons of z-transformed and age-corrected group means of the relative and absolute parahippocampal integrity measurements indicate the superiority of the CSR in the matter of differentiating older adults with cognitively normal (CN), MCI and AD. On the one hand, the relative integrity group means mainly assume more extreme values compared to the absolute integrity. This indicates that these subgroups can be distinguished more clearly from each other. On the other hand, it is of crucial interest that only when considering the CSR, the expected group order in terms of parahippocampal integrity is sustained. These findings are consistent with the hypothesis and could be statistically verified by significant interactions with large effect sizes in mixed covariance analyses, controlling for age, for the left perirhinal cortex (PRC), entorhinal cortex (EC) and total PHG. There were no significant interactions for the examined structures of the right hemisphere. Although the interaction of the right parhippocampal cortex (PHC) reached marginal significance, it must be considered that the expected group order of parahippocampal integrity for age-adjusted group means of the CSR was not maintained for this structure. Compared to the overall mean, the MCI sample showed even lower CSR values for the right PHC than AD-patients.

CSR indicates parahippocampal changes in MCI and AD

In accordance with histopathological findings that revealed an early involvement of parahippocampal structures in AD pathogenesis with EC and PRC being the first to be damaged (Braak & Braak, 1991; van Hoesen et al., 2000), a number of studies showed that early structural changes in parahippocampal volume can be detected using MRI. Various cross-sectional & longitudinal MRI-studies demonstrated grey matter reductions in EC and PRC associated with AD (Busatto et al., 2003; Juottonen et al., 1998; Krumm et al., 2016; Schmidt-Wilcke, Poljansky, Hierlmeier, Hausner & Ibach, 2009). A meta-analysis by Wang et al. (2015) showed that individuals with AD had significantly smaller regional grey matter volume in the left PHG compared to those that are CN. A similar meta-analysis of longitudinal studies conducted by

Ferreira, Diniz, Forlenza, Busatto and Zanetti (2011) revealed a significant cluster of grey matter volume reduction in the left PHG in MCI-patients who converted to AD. These meta-analyses indicate the robustness of volume reduction in the left PHG in the context of AD.

Regarding the relative parahippocampal integrity measure the current results align with the pattern of evidence that showed grey matter reductions in the PHG, most consistently in the left hemisphere. Concluding from the statistical analysis and descriptive comparisons, when considering age as a covariate, the CSR reveals differences between CN, MCI and AD individuals in the integrity of their left PHG in total as well as their left EC and PRC when inspected separately. In this context, it is important to note that the significant result for the overall marker may probably be largely due to structural changes of the PRC and EC. Since particularly EC and PRC appear to be the first affected by the pathological processes of AD, examining their integrity seems to be on target in terms of estimating the development of AD even in early stages. Thus, as also implied by previous research, estimating the integrity of parahippocampal structures, especially the left PRC and EC, can be a valuable biomarker to differentiate subjects with and without AD and maybe to identify people with risk for developing AD.

Overcome weaknesses of existing markers to increase promising utility

In general, medial temporal lobe (MTL) atrophy on MRI is regarded to be the furthest through validation process as it is the only biomarker for which a plenty of evidence is available for its rational use and early discriminative ability between diseased and control subjects (Frisoni et al., 2017; Ten Kate et al., 2017). Yet, researchers claim there is not enough systematically addressed evidence to implement this biomarker for early diagnosis in practice and its clinical utility is considered insufficient (Frisoni, Hampel, O'Brien, Ritchie & Winblad, 2011; Frisoni et al., 2017; Scheltens et al., 2021; Ten Kate et al., 2017).

According to Frisoni et al. (2017) clinical utility of MTL atrophy has among other things been weakened by methodological differences in study designs as heterogeneous reference populations have been used to establish normative values and differences in measurements have led to no thresholds for positivity in volumetric analysis yet being validated. The effects of different methodological approaches were also observed in the present study: Although manual segmentation of the MRI-brains was largely based on the work of Pruessner et al. (2002), substantial differences were detected between studies in the uncorrected absolute cortical volumes, which has been used by default in previous studies to estimate parahippocampal integrity. While it seems plausible that using different segmentation protocols increases the variance between study results in general, in terms of PHG volumetry it is also particularly important to consider the variability of the PHG in general population. As for instance evidence suggests that parahippocampal volume loss occurs as a result of normal aging (Sele et al., 2021) among other developmental predispositions, the composition of the sample is one thing that has to be kept in mind when comparing cross-sectional study results regarding par-ahippocampal integrity. Bivariate subordinated analyses underscore this fact: the absolute cortical volume used by default to assess parahippocampal integrity showed moderate to high negative associations with age. Another major weakness of MRI biomarkers assessing MTL atrophy is the limited accuracy when they are used alone. In the case of the PHG, a review by Atiya, Hyman, Albert & Killiany (2003) states that although the PHG is among the most affected structure in patients with AD, used alone it is unable to discriminate subjects with a satisfactory accuracy.

Overcoming these weaknesses of existing markers could be beneficial from a clinical perspective taking into account the delayed onset of pathophysiology and clinical manifestation. An optimised MRI-based biomarker reflecting the underlying AD pathology early could presumably represent an important opportunity for early identification of risk patients and for prognosing and monitoring disease progression, and consequently reduce the burden on specialists and create a time window for early treatment (Pornsteinsson, Isaacson, Knox, Sabbagh & Rubino, 2021; Schmand et al. 2010). The National Institute on Aging - Alzheimer's Association introduced the use of biomarkers for the diagnosis of AD and recommends their use for the detection of AD in subjects with MCI (Albert et al., 2013). Considering the body of evidence suggesting that structural changes in PHG can be detected early, refining the measurement of the PHG integrity could help to in-crease the clinical utility of MRI-based biomarkers in early AD detection. A particularly important point, which has so far received little attention in the context of estimating parahippocampal integrity, is the huge variability in the appearance of the PHG.

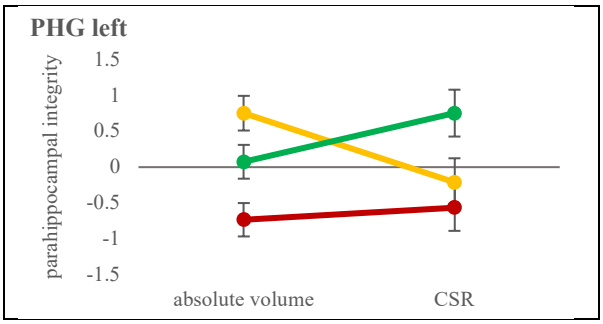

*Figure 4.*1. Age-adjusted *M*±*SD* for the integrity measures of the left total parahippocampal gyrus (PHG). *N*=23.

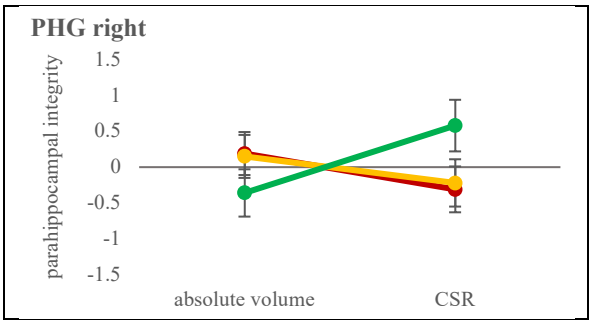

Figure 4.2. Age-adjusted *M*±*SD* for the integrity measures of the right total parahippocampal gyrus (PHG). *N*=22.

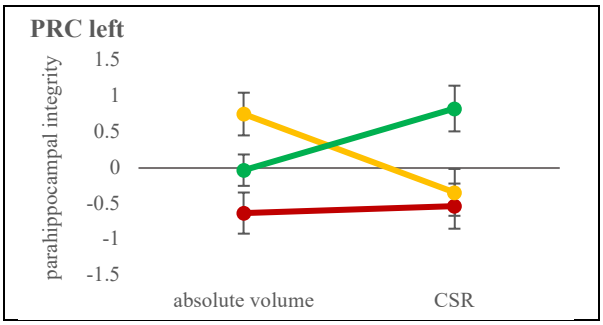

Figure 4.3. Age-adjusted *M*±*SD* for the integrity measures of the left perirhinal cortex (PRC). *N*=23.

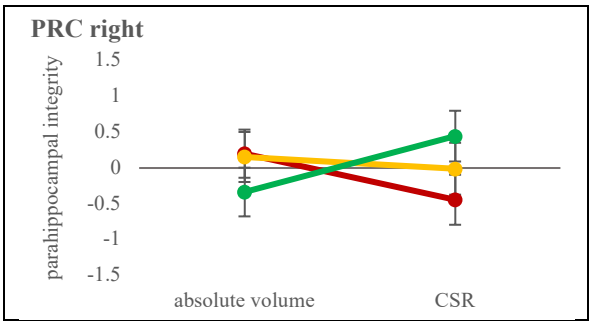

Figure 4.4. Age-adjusted *M*±*SD* for the integrity measures of the right perirhinal cortex (PRC). *N*=23.

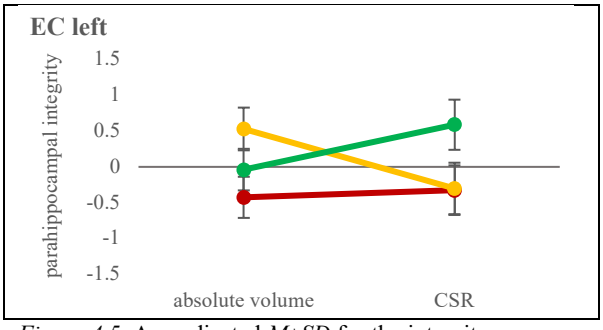

Figure 4.5. Age-adjusted *M*±*SD* for the integrity measures of the left entorhinal cortex (EC). *N*=23.

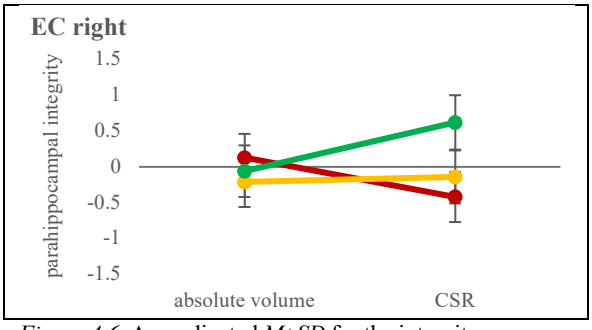

Figure 4.6. Age-adjusted *M*±*SD* for the integrity measures of the right entorhinal cortex (EC). *N*=22.

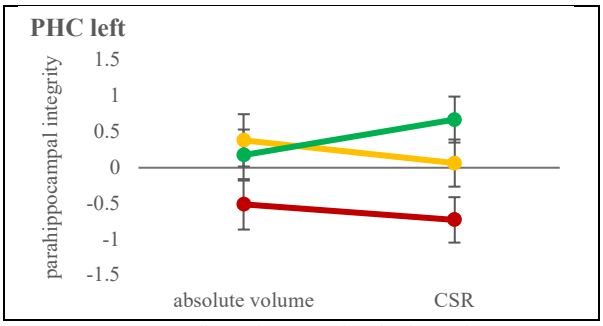

Figure 4.7. Age-adjusted *M*±*SD* for the integrity measures of the left parahippocampal cortex (PHC). *N*=23.

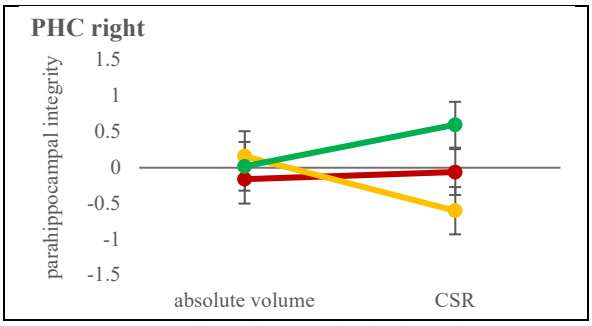

Figure 4.8. Age-adjusted *M*±*SD* for the integrity measures of the right parahippocampal cortex (PHC). *N*=23.

Alzheimer's disease Mild cognitive impairment Cognitively normal

Figure 4. Interaction plots with age-adjusted values of the parahippocampal integrity separated by hemisphere and parahippocampal structure. Each point represents an z-transformed, age-adjusted group mean of the absolute volume or the CSR operationalising the different integrity measures. A solid grey line with y=0 marks the overall mean. Different group levels are presented in distinct colours. Nonparallel lines indicate an interaction of the between factor group and the within factor integrity measurement. CSR=Cortex-to-Sulcus-Ratio.

To rephrase it, a small PHG may exist due to various influencing factors rather than an underlying AD pathology. The large variation in parahippocampal volumes in the general population thus limits the assessment of parahippocampal integrity from absolute volumetric cross-sectional MRI data.

Benefits of refining the estimation of parahippocampal integrity by including a measurement of sulcal enlargement

By including a volumetric measurement of the CS, which is embedded in the PHG, to the standardly used absolute volumetric measure of the parahippocampal grey matter, it was assumed that the CSR would overcome the effects of parahippocampal variability in general population. This new relative measurement for parahippocampal integrity was believed to allow for a better discrimination of volumetric changes from developmental variations in parahippocampal volume and thus to increase the clinical utility as AD-biomarker. On the one hand, the results show that using the CSR, especially in case of the left PRC and EC, ensures a differentiation of individuals with CN, MCI and AD, when age is considered as a covariate. On the other hand, in contrast to most previous studies that rely on absolute volumetric measurements, this could not be shown when looking at this standardly used estimation of cortical integrity. Moreover, the absolute parahippocampal volumes showed stronger associations with the individual's age. These aspects underscore the criticism of lacking accuracy and dependency on other influencing factors. Overall, the results imply that the CSR may be a more sensitive marker for AD related changes in parahippocampal integrity than absolute cortical volumes and therefore indicate the hypothesised superiority of this relative measurement for parahippocampal integrity when estimating AD development.

Combining the measurements of cortical volume and the extension of the CS thus appears to be of significant value in this regard. Previous studies investigating the utility of measuring changes in sulcal shapes in diagnosing AD showed that sulcal morphology is affected by AD atrophy and indicates differences between CN and AD-subjects (Andersen et al., 2015; Hamelin et al., 2015; Im et al., 2008). Although there is little specific research on the CS in this context, for example Juottonen et al. (1998) found that the CS is expanded in people with AD compared to healthy controls. Recognising the enlargement of cerebrospinal fluid compartments as a result of brain atrophy, relating rates of cortical atrophy and cerebrospinal fluid compartments may result in ratios with additional potential to absolute volumes in AD (Bartos, Gregus, Ibrahim & Tintěra, 2019; Wang & Doddrell, 2002). Based on this concept some studies presented ratios for other struc-tures than the PHG and demonstrated their improved ability to distinguish AD-patients and age-matched controls (Bartos et al., 2019; Wang & Doddrell, 2002; Wang et al., 2002). The implementation of such a ratio estimating the integrity of the PHG in the current study is largely adapted from the method of Schoemaker et al. (2019) estimating the relative hippocampal integrity. Their findings support an added benefit of using the Hippocampal-to-Ventricle-Ratio over standard hippocampal volume when evaluating the hippocampal integrity from cross-sectional MRI. This is the first study to transfer the idea of a relative integrity measure to the PHG by generating the CSR. Since there are no studies available that examined a combination of cortical and sulcal volume in terms of the PHG, directly contrasting effect sizes or a comparison of the CSR with other ratios estimating parahippocampal integrity cannot be performed. However, cautiously daring a comparison with a study examining atrophy rates in the region of temporal lobes measured on serially acquired T1-weighted brain MRI, results align in the sense that by accounting for cortical atrophy and cerebrospinal fluid compartments significant differences between AD-patients and age-matched CN subjects can be detected (Wang & Doddrell, 2002; Wang et al., 2002). Wang et al. (2002) interpreted their results in the sense that relating these measurements can provide sensitive evaluations of the progression of AD. Carefully applying this conclusion to the PHG, implies that the CSR could not only be a valuable biomarker to differentiate groups but potentially identifies individuals at risk for developing AD.

Major advantages, limitations and recommendations for future research

This exploratory study took a first step towards validation of a relative measurement of parahippocampal integrity as a potentially useful biomarker for early detection of AD. In terms of the PHG, the CSR has been the first assessment, which considers the volumetric relationship of its cortical structures and the adjacent CS. This ratio offers some advantages over the previously used standard absolute volume to assess the PHG integrity. Most importantly, accounting for the CS corrects for anatomical variability

which has largely decreased the usefulness of earlier biomarkers. Bartos et al. (2019) claim that by relating opposing structures the influence of further factors may be reduced. The present study provides initial evidence for the CSR being less dependent on age than the absolute cortical volume. However, since this was not a primary objective of the study, further investigations are required to make reliable statements. Another fundamental advantage over absolute volumes is the self-explanatory nature of the CSR. This integrity index can only assume values between 0 and 1 and is a direct reflection of the neurodegeneration of the PHG. Although reference norms are not necessary to understand the basic meaning, they could be useful to figure out regular variations with age and thus detect unusual parahippocampal neurodegeneration at an individual level.

Despite the encouraging aspects, some limitations of the study must also be considered. On the one hand, the methodological implementation can be criticised for analysing a relatively small sample and for not including any cognitive variables, which might depict the continuum of the disease more accurately than categorical diagnosis. From this point of view, it must be taken into account that larger CSR values of individual subjects in the CN sample could indicate AD-related pathological changes are already recognisable while they are not yet cognitively detectable. On the other hand, the lack of information on additional sample characteristics such as gender, level of education or the presence of comorbidities also limits the generalisability of the results. In general, using manual segmentation is known for being laborious, as it cannot be carried out by laypersons and is very time consuming (Ten Kate et al., 2017). However, before work is put into semi- or fully automated segmentation protocols, which would facilitate application in larger sample sizes and across laboratories, the current results should be replicated first. Delayed verifications from longitudinal data of CN subjects that develop MCI due to AD could also help to demonstrate the relevance of the CSR. Overall, it should be noted that at the present time it cannot be guaranteed that the CSR can validly detect AD at prodromal stage before clinical symptoms manifest. According to Schmand et al. (2010) this would imply that the prognostic accuracy of this biomarker is clearly superior to measures of behavioural symptoms. Future research is needed to verify these claims and to further validate the use of relative parahippocampal integrity in clinical practice.

Frisoni et al. (2017) summarised interdisciplinary conclusions and recommendations to promote the adoption of biomarkers for an early diagnosis of AD in clinical practice. They presented a strategic five-phase roadmap which requires that a phase is addressed only after the previous ones have been completed. The current study provides evidence for the ability of the CSR to distinguish individuals with and without AD. As this is a primary goal for clinical assay development according to Frisoni et al. (2017), it can be seen as a door opener towards clinical validity. In agreement with the framework next research steps to evaluate the CSR should address the frequency of true-positive and false-positive results, as well as secondary aims such as the assessment of variables associated with the biomarker status or the exploration of the impact of covariates on discriminatory abilities.

Appendix

Supplementary information is available at the end of this article.

References

Albert, M. S., DeKosky, S. T., Dickson, D., Dubois, B., Feldman, H. H., Fox, N. C., ... & Phelps, C. H. (2013). The diagnosis of mild cognitive impairment due to Alzheimer's disease: recommendations from the National Institute on Aging-Alzheimer's Association workgroups on diagnostic guidelines for Alzheimer's disease. *Focus*, *11*(1), 96-106. https://doi.org/10.1176/appi.focus.11.1.96

Andersen, S. K., Jakobsen, C. E., Pedersen, C. H., Rasmussen, A. M., Plocharski, M. & Østergaard, L. R. (2015). Classification of Alzheimer's disease from MRI using sulcal morphology. In R. R. Paulsen & K. S. Pedersen (Eds.) *Image Analysis. 19th Scandinavian Conference, SCIA 2015, Copenhagen, Denmark, June 15-17, 2015. Proceedings* (pp. 103-113). Springer. https://doi.org/10.1007/978-3-319-19665-7

Atiya, M., Hyman, B. T., Albert, M. S. & Killiany, R. (2003). Structural magnetic resonance imaging in established and prodromal Alzheimer disease: a review. *Alzheimer Disease & Associated Disorders*, *17*(3), 177-195. https://doi.org/10.1097/00002093-200307000-00010

Augustinack, J. C., van der Kouwe, A. J. & Fischl, B. (2013). Medial temporal cortices in ex vivo magnetic resonance imaging. *Journal of Comparative Neurology*, *521*(18), 4177-4188. https://doi.org/10.1002/cne.23432

Bartos, A., Gregus, D., Ibrahim, I. & Tintěra, J. (2019). Brain volumes and their ratios in Alzheimer s disease on magnetic resonance imaging segmented using Freesurfer 6.0. *Psychiatry Research: Neuroimaging*, *287*, 70-74. https://doi.org/10.1016/j.pscychresns.2019.01.014

Beekly, D. L., Ramos, E. M., Lee, W. W., Deitrich, W. D., Jacka, M. E., Wu, J., ... & Kukull, W. A. (2007). The National Alzheimer's Coordinating Center (NACC) database: the uniform data set. *Alzheimer Disease & Associated Disorders*, *21*(3), 249-258. https://doi.org/10.1097/WAD.0b013e318142774e

Box, G. E. (1949). A general distribution theory for a class of likelihood criteria. *Biometrika*, *36*(3/4), 317-346. https://doi.org/10.2307/2332671

Braak, H. & Braak, E. (1991). Neuropathological stageing of Alzheimer-related changes. *Acta neuropathologica*, *82*(4), 239-259. https://doi.org/10.1007/BF00308809

Braak, H., Braak, E. & Bohl, J. (1993). Staging of Alzheimer-related cortical destruction. *European neurology*, *33*(6), 403-408. https://doi.org/10.1159/000116984

Busatto, G. F., Garrido, G. E., Almeida, O. P., Castro, C. C., Camargo, C. H., Cid, C. G., ... & Bottino, C. M. (2003). A voxel-based morphometry study of temporal lobe gray matter reductions in Alzheimer's disease. *Neurobiology of aging*, *24*(2), 221-231. https://doi.org/10.1016/S0197-4580(02)00084-2

Chao, L. L., Mueller, S. G., Buckley, S. T., Peek, K., Raptentsetseng, S., Elman, J., ... & Weiner, M. W. (2010). Evidence of neurodegeneration in brains of older adults who do not yet fulfill MCI criteria. *Neurobiology of aging*, *31*(3), 368-377. https://doi.org/10.1016/j.neurobiolaging.2008.05.004

Cohen, J. (1988). *Statistical power analysis for the behavioral sciences* (2nd ed.). Hillsdale, NJ: Erlbaum. https://dx.doi.org/10.4324/9780203771587

Collins, D. L., Neelin, P., Peters, T. M. & Evans, A. C. (1994). Automatic 3D intersubject registration of MR volumetric data in standardized Talairach space. *Journal of computer assisted tomography*, *18*(2), 192-205.

Coupé, P., Eskildsen, S. F., Manjón, J. V., Fonov, V. S., Collins, D. L. & Alzheimer's Disease Neuroimaging Initiative. (2012). Simultaneous segmentation and grading of anatomical structures for patient's classification: application to Alzheimer's disease. *NeuroImage*, *59*(4), 3736-3747. https://doi.org/10.1016/j.neuroimage.2011.10.080

Coupé, P., Yger, P., Prima, S., Hellier, P., Kervrann, C. & Barillot, C. (2008). An optimized blockwise nonlocal means denoising filter for 3-D magnetic resonance images. *IEEE transactions on medical imaging*, *27*(4), 425-441. https://doi.org/10.1109/TMI.2007.906087

De Leon, M. J., Convit, A., DeSanti, S., Bobinski, M., George, A. E., Wisniewski, H. M., ... & Saint Louis, L. A. (1997). Contribution of structural neuroimaging to the early diagnosis of Alzheimer's disease. *International Psychogeriatrics*, *9*(S1), 183-190. https://doi.org/10.1017/S1041610297004900

De Strooper, B. & Karran, E. (2016). The cellular phase of Alzheimer's disease. *Cell*, *164*(4), 603-615. https://doi.org/10.1016/j.cell.2015.12.056

De Toledo-Morrell, L., Goncharova, I., Dickerson, B., Wilson, R. S. & Bennett, D. A. (2000). From healthy aging to early Alzheimer's disease: in vivo detection of entorhinal cortex atrophy. *Annals of the New York Academy of Sciences*, *911*(1), 240-253. https://doi.org/10.1111/j.1749-6632.2000.tb06730.x

DeTure, M. A. & Dickson, D. W. (2019). The neuropathological diagnosis of Alzheimer's disease. *Molecular neurodegeneration*, *14*(1), 1-18. https://doi.org/10.1186/s13024-019-0333-5

Devanand, D. P., Bansal, R., Liu, J., Hao, X., Pradhaban, G., & Peterson, B. S. (2012). MRI hippocampal and entorhinal cortex mapping in predicting conversion to Alzheimer's disease. *Neuroimage*, *60*(3), 1622-1629. https://doi.org/10.1016/j.neuroimage.2012.01.075

Dickerson, B. C., Goncharova, I., Sullivan, M. P., Forchetti, C., Wilson, R. S., Bennett, D. A., ... & deToledo-Morrell, L. (2001). MRI-derived entorhinal and hippocampal atrophy in incipient and very mild Alzheimer's disease. *Neurobiology of aging*, *22*(5), 747-754. https://doi.org/10.1016/S0197-4580(01)00271-8

Ebenau, J. L., Timmers, T., Wesselman, L. M., Verberk, I. M., Verfaillie, S. C., Slot, R. E., ... & Van Der Flier, W. M. (2020). ATN classification and clinical progression in subjective cognitive decline: The SCIENCe project. *Neurology*, *95*(1), e46-e58. https://doi.org/10.1212/WNL.0000000000009724

Echávarri, C., Aalten, P., Uylings, H. B., Jacobs, H. I. L., Visser, P. J., Gronenschild, E. H. B. M., ... & Burgmans, S. (2011). Atrophy in the parahippocampal gyrus as an early biomarker of Alzheimer's disease. *Brain Structure and Function*, *215*(3), 265-271. https://doi.org/10.1007/s00429-010-0283-8

Federer, W. T. & Meredith, M. P. (1992). Covariance analysis for split-plot and split-block designs. *The American Statistician*, *46*(2), 155-162. https://doi.org/10.1080/00031305.1992.10475875

Ferreira, L. K., Diniz, B. S., Forlenza, O. V., Busatto, G. F. & Zanetti, M. V. (2011). Neurostructural predictors of Alzheimer's disease: a meta-analysis of VBM studies. *Neurobiology of aging*, *32*(10), 1733-1741. https://doi.org/10.1016/j.neurobiolaging.2009.11.008.

Field, A. (2013). *Discovering statistics using IBM SPSS statistics: and sex and drugs and rock 'n' roll* (4th ed.). Los Angeles: Sage.

Frisoni, G. B., Boccardi, M., Barkhof, F., Blennow, K., Cappa, S., Chiotis, K., ... & Winblad, B. (2017). Strategic roadmap for an early diagnosis of Alzheimer's disease based on biomarkers. *The Lancet Neurology*, *16*(8), 661-676. https://doi.org/10.1016/S1474-4422(17)30159-X

Frisoni, G. B., Fox, N. C., Jack, C. R., Scheltens, P. & Thompson, P. M. (2010). The clinical use of structural MRI in Alzheimer disease. *Nature Reviews Neurology*, *6*(2), 67-77. https://doi.org/10.1038/nrneurol.2009.215

Frisoni, G. B., Hampel, H., T O'Brien, J., Ritchie, K. & Winblad, B. (2011). Revised criteria for Alzheimer's disease: what are the lessons for clinicians?. *The Lancet Neurology*, *10*(7), 598-601. https://doi.org/10.1016/S1474-4422(11)70126-0

Hamelin, L., Bertoux, M., Bottlaender, M., Corne, H., Lagarde, J., Hahn, V., ... & Sarazin, M. (2015). Sulcal morphology as a new imaging marker for the diagnosis of early onset Alzheimer's disease. *Neurobiology of aging*, *36*(11), 2932-2939. https://doi.org/10.1016/j.neurobiolaging.2015.04.019

IBM Corp. (2022). IBM SPSS Statistics for Windows, version 29.0. *Armonk, NY: IBM Corp.*

Im, K., Lee, J. M., Seo, S. W., Kim, S. H., Kim, S. I. & Na, D. L. (2008). Sulcal morphology changes and their relationship with cortical thickness and gyral white matter volume in mild cognitive impairment and Alzheimer's disease. *Neuroimage*, *43*(1), 103-113. https://doi.org/10.1016/j.neuroimage.2008.07.016

Insausti, R., Juottonen, K., Soininen, H., Insausti, A. M., Partanen, K., Vainio, P., ... & Pitkänen, A. (1998). MR volumetric analysis of the human entorhinal, perirhinal, and temporopolar cortices. *American journal of neuroradiology*, *19*(4), 659-671.

Jack Jr, C. R., Bennett, D. A., Blennow, K., Carrillo, M. C., Dunn, B., Haeberlein, S. B., ... & Silverberg, N. (2018). NIA-AA research framework: toward a biological definition of Alzheimer's disease. *Alzheimer's & Dementia*, *14*(4), 535-562. https://doi.org/10.1016/j.jalz.2018.02.018

Jack Jr, C. R., Knopman, D. S., Weigand, S. D., Wiste, H. J., Vemuri, P., Lowe, V., ... & Petersen, R. C. (2012). An operational approach to National Institute on Aging–Alzheimer's Association criteria for preclinical Alzheimer disease. *Annals of neurology*, *71*(6), 765-775. https://doi.org/10.1002/ana.22628

Jack, C. R., Shiung, M. M., Weigand, S. D., O'brien, P. C., Gunter, J. L., Boeve, B. F., ... & Petersen, R. C. (2005). Brain atrophy rates predict subsequent clinical conversion in normal elderly and amnestic MCI. *Neurology*, *65*(8), 1227-1231. https://doi.org/10.1212/01.wnl.0000180958.22678.91

Juottonen, K., Laakso, M. P., Insausti, R., Lehtovirta, M., Pitkänen, A., Partanen, K. & Soininen, H. (1998). Volumes of the entorhinal and perirhinal cortices in Alzheimer's disease. *Neurobiology of aging*, *19*(1), 15-22. https://doi.org/10.1016/S0197-4580(98)00007-4

Kesslak, J. P., Nalcioglu, O. & Cotman, C. W. (1991). Quantification of magnetic resonance scans for hippocampal and parahippocampal atrophy in Alzheimer's disease. *Neurology*, *41*(1), 51-51. https://doi.org/10.1212/WNL.41.1.51

Killiany, R. J., Gomez-Isla, T., Moss, M., Kikinis, R., Sandor, T., Jolesz, F., ... & Albert, M. S. (2000). Use of structural magnetic resonance imaging to predict who will get Alzheimer's disease. *Annals of Neurology: Official Journal of the American Neurological Association and the Child Neurology Society*, *47*(4), 430-439. https://doi.org/10.1002/1531-8249(200004)47:4%3C430::AID-ANA5%3E3.0.CO;2-I

Köhler, S., Black, S. E., Sinden, M., Szekely, C., Kidron, D., Parker, J. L., ... & Bronskill, M. J. (1998). Memory impairments associated with hippocampal versus parahippocampal-gyrus atrophy: an MR volumetry study in Alzheimer's disease. *Neuropsychologia*, *36*(9), 901-914. https://doi.org/10.1016/S0028-3932(98)00017-7

Krumm, S., Kivisaari, S. L., Probst, A., Monsch, A. U., Reinhardt, J., Ulmer, S., ... & Taylor, K. I. (2016). Cortical thinning of parahippocampal subregions in very early Alzheimer's disease. *Neurobiology of aging*, *38*, 188-196. https://doi.org/10.1016/j.neurobiolaging.2015.11.001

LaMontagne, P. J., Benzinger, T. L., Morris, J. C., Keefe, S., Hornbeck, R., Xiong, C., ... & Marcus, D. (2019). OASIS-3: longitudinal neuroimaging, clinical, and cognitive dataset for normal aging and Alzheimer disease. *MedRxiv*. https://doi.org/10.1101/2019.12.13.19014902

Lawrence, V., Pickett, J., Ballard, C. & Murray, J. (2014). Patient and carer views on participating in clinical trials for prodromal Alzheimer's disease and mild cognitive impairment. *International journal of geriatric psychiatry*, *29*(1), 22-31. https://doi.org/10.1002/gps.3958

McKhann, G.M., Drachman, D., Folstein, M., Katzman, R., Price, D. & Stadlan, E. M. (1984). Clinical diagnosis of Alzheimer's disease: Report of the NINCDS-ADRDA Work Group under the auspices of Department of Health and Human Services Task Force on Alzheimer's Disease. *Neurology*, *34*(7), 939-939. https://doi.org/10.1212/WNL.34.7.939

McKhann, G. M., Knopman, D. S., Chertkow, H., Hyman, B. T., Jack Jr, C. R., Kawas, C. H., ... & Phelps, C. H. (2011). The diagnosis of dementia due to Alzheimer's disease: Recommendations from the National Institute on Aging-Alzheimer's Association workgroups on diagnostic guidelines for Alzheimer's disease. *Alzheimer's & dementia*, *7*(3), 263-269. https://doi.org/10.1016/j.jalz.2011.03.005

Meda, S. A., Hawkins, K. A., Dager, A. D., Tennen, H., Khadka, S., Austad, C. S., ... & Pearlson, G. D. (2018). Longitudinal effects of alcohol consumption on the hippocampus and parahippocampus in college students. *Biological Psychiatry: Cognitive Neuroscience and Neuroimaging*, *3*(7), 610-617. https://doi.org/10.1016/j.bpsc.2018.02.006

Miller, G. A. & Chapman, J. P. (2001). Misunderstanding analysis of covariance. *Journal of abnormal psychology*, *110*(1), 40-48. https://doi.org/10.1037//0021-843X.110.1.40

Morris, J. C. (1993). The Clinical Dementia Rating (CDR): current version and scoring rules. *Neurology, 43*(11), 2412–2414 (1993). https://doi.org/10.1212/wnl.43.11.2412-a

Morris, J. C. (1997). Clinical dementia rating: a reliable and valid diagnostic and staging measure for dementia of the Alzheimer type. *International psychogeriatrics*, *9*(S1), 173-176. https://doi.org/10.1017/S1041610297004870

Morris, J. C., Weintraub, S., Chui, H. C., Cummings, J., DeCarli, C., Ferris, S., ... & Kukull, W. A. (2006). The Uniform Data Set (UDS): clinical and cognitive variables and descriptive data from Alzheimer Disease Centers. *Alzheimer Disease & Associated Disorders*, *20*(4), 210-216. https://doi.org/10.1097/01.wad.0000213865.09806.92

Mosconi, L., Brys, M., Glodzik-Sobanska, L., De Santi, S., Rusinek, H. & De Leon, M. J. (2007). Early detection of Alzheimer's disease using neuroimaging. *Experimental gerontology*, *42*(1-2), 129-138. https://doi.org/10.1016/j.exger.2006.05.016

Pantel, J., Hüger, D. R., Kratz, B., Minnemann, E., Martin, M., Schad, L. R., ... & Schröder, J. (2002). Strukturelle zerebrale Veränderungen bei Probanden mit leichter kognitiver Beeinträchtigung Eine MR-volumetrische Studie. *Der Nervenarzt*, *73*(9), 845-850. https://doi.org/10.1007/s001150101154

Petersen, R. C., Doody, R., Kurz, A., Mohs, R. C., Morris, J. C., Rabins, P. V., ... & Winblad, B. (2001). Current concepts in mild cognitive impairment. *Archives of neurology*, *58*(12), 1985-1992. https://doi.org/10.1001/archneur.58.12.1985

Petersen, R. C., Smith, G. E., Waring, S. C., Ivnik, R. J., Tangalos, E. G. & Kokmen, E. (1999). Mild cognitive impairment: clinical characterization and outcome. *Archives of neurology*, *56*(3), 303-308. https://doi.org/10.1001/archneur.56.3.303

Pituch, K. A. & Stevens, J. P. (2016). *Applied multivariate statistics for the social sciences: analyses with SAS and IBM's SPSS* (6th ed.). New York: Routledge. https://doi.org/10.4324/9781315814919

Porsteinsson, A. P., Isaacson, R. S., Knox, S., Sabbagh, M. N. & Rubino, I. (2021). Diagnosis of early alzheimer's disease: Clinical practice in 2021. *The Journal of Prevention of Alzheimer's Disease*, *8*(3), 371-386. https://doi.org/10.14283/jpad.2021.23

Pruessner, J. C., Köhler, S., Crane, J., Pruessner, M., Lord, C., Byrne, A., ... & Evans, A. C. (2002). Volumetry of temporopolar, perirhinal, entorhinal and parahippocampal cortex from high-resolution MR images: considering the variability of the collateral sulcus. *Cerebral Cortex*, *12*(12), 1342-1353. https://doi.org/10.1093/cercor/12.12.1342

Pruessner, J. C., Li, L. M., Serles, W., Pruessner, M., Collins, D. L., Kabani, N., ... & Evans, A. C. (2000). Volumetry of hippocampus and amygdala with high-resolution MRI and three-dimensional analysis software: minimizing the discrepancies between laboratories. *Cerebral cortex*, *10*(4), 433-442. https://doi.org/10.1093/cercor/10.4.433

Raskin, J., Cummings, J., Hardy, J., Schuh, K. & A Dean, R. (2015). Neurobiology of Alzheimer's disease: integrated molecular, physiological, anatomical, biomarker, and cognitive dimensions. *Current Alzheimer Research*, *12*(8), 712-722. https://doi.org/10.2174/1567205012666150701103107

Raslau, F. D., Mark, I. T., Klein, A. P., Ulmer, J. L., Mathews, V. & Mark, L. P. (2015). Memory part 2: the role of the medial temporal lobe. *American Journal of Neuroradiology*, *36*(5), 846-849. https://doi.org/10.3174/ajnr.A4169

Scheltens, P., De Strooper, B., Kivipelto, M., Holstege, H., Chételat, G., Teunissen, C. E., ... & van der Flier, W. M. (2021). Alzheimer's disease. *The Lancet*, *397*(10284), 1577-1590. https://doi.org/10.1016/S0140-6736(20)32205-4

Schmand, B., Huizenga, H. M. & Van Gool, W. A. (2010). Meta-analysis of CSF and MRI biomarkers for detecting preclinical Alzheimer's disease. *Psychological Medicine*, *40*(1), 135-145. https://doi.org/10.1017/S0033291709991516

Schmidt-Wilcke, T., Poljansky, S., Hierlmeier, S., Hausner, J. & Ibach, B. (2009). Memory performance correlates with gray matter density in the ento-/perirhinal cortex and posterior hippocampus in patients with mild cognitive impairment and healthy controls—a voxel based morphometry study. *Neuroimage*, *47*(4), 1914-1920. https://doi.org/10.1016/j.neuroimage.2009.04.092

Schoemaker, D., Buss, C., Pietrantonio, S., Maunder, L., Freiesleben, S. D., Hartmann, J., ... & Pruessner, J. C. (2019). The hippocampal-to-ventricle ratio (HVR): presentation of a manual segmentation protocol and preliminary evidence. *Neuroimage*, *203*, 116108. https://doi.org/10.1016/j.neuroimage.2019.116108

Schultz, C., Del Tredici, K. & Braak, H. (2004). Neuropathology of Alzheimer's Disease. In: R. W. Richter & B. Z. Richter (Eds.) *Alzheimer's Disease. A Physician's Guide to Practical Management* (pp. 21-31). Totowa, NJ: Humana Press. https://doi.org/10.1007/978-1-59259-661-4

Sele, S., Liem, F., Mérillat, S. & Jäncke, L. (2021). Age-related decline in the brain: a longitudinal study on inter-individual variability of cortical thickness, area, volume, and cognition. *Neuroimage*, *240*, 118370. https://doi.org/10.1016/j.neuroimage.2021.118370

Sled, J. G., Zijdenbos, A. P. & Evans, A. C. (1998). A nonparametric method for automatic correction of intensity nonuniformity in MRI data. *IEEE transactions on medical imaging*, *17*(1), 87-97. https://doi.org/10.1109/42.668698

Ten Kate, M., Barkhof, F., Boccardi, M., Visser, P. J., Jack Jr, C. R., Lovblad, K. O., ... & for the Roadmap, G. T. F. (2017). Clinical validity of medial temporal atrophy as a biomarker for Alzheimer's disease in the context of a structured 5-phase development framework. *Neurobiology of aging*, *52*, 167-182. https://doi.org/10.1016/j.neurobiolaging.2016.05.024

Twamley, E. W., Ropacki, S. A. L. & Bondi, M. W. (2006). Neuropsychological and neuroimaging changes in preclinical Alzheimer's disease. *Journal of the International Neuropsychological Society*, *12*(5), 707-735. https://doi.org/10.1017/s1355617706060863

van Hoesen, G. W., Augustinack, J. C., Dierking, J., Redman, S. J. & Thangavel, R. (2000). The parahippocampal gyrus in Alzheimer's disease: clinical and preclinical neuroanatomical correlates. *Annals of the New York Academy of Sciences*, *911*(1), 254-274. https://doi.org/10.1111/j.1749-6632.2000.tb06731.x

van Maurik, I. S., Vos, S. J., Bos, I., Bouwman, F. H., Teunissen, C. E., Scheltens, P., ... & Alzheimer's Disease Neuroimaging Initiative. (2019). Biomarker-based prognosis for people with mild cognitive impairment (ABIDE): a modelling study. *The Lancet Neurology*, *18*(11), 1034-1044. https://doi.org/10.1016/S1474-4422(19)30283-2

Visser, P. J., Scheltens, P., Verhey, F. R., Schmand, B., Launer, L. J., Jolles, J. & Jonker, C. (1999). Medial temporal lobe atrophy and memory dysfunction as predictors for dementia in subjects with mild cognitive impairment. *Journal of neurology*, *246*(6), 477-485. https://doi.org/10.1007/s004150050387

Wang, D. & Doddrell, D. M. (2002). MR image-based measurement of rates of change in volumes of brain structures. Part I: method and validation. *Magnetic resonance imaging*, *20*(1), 27-40. https://doi.org/10.1016/S0730-725X(02)00466-6

Wang, D., Chalk, J. B., Rose, S. E., de Zubicaray, G., Cowin, G., Galloway, G. J., ... & Semple, J. (2002). MR image-based measurement of rates of change in volumes of brain structures. Part II: application to a study of Alzheimer's disease and normal aging. *Magnetic resonance imaging*, *20*(1), 41-48. https://doi.org/10.1016/S0730-725X(02)00472-1

Wang, W. Y., Yu, J. T., Liu, Y., Yin, R. H., Wang, H. F., Wang, J., ... & Tan, L. (2015). Voxel-based meta-analysis of grey matter changes in Alzheimer's disease. *Translational neurodegeneration*, *4*, 6. https://doi.org/10.1186/s40035-015-0027-z

Zhou, H., Li, R., Ma, Z., Rossi, S., Zhu, X. & Li, J. (2016). Smaller gray matter volume of hippocampus/parahippocampus in elderly people with subthreshold depression: a cross-sectional study. *BMC psychiatry*, *16*(1), 219. https://doi.org/10.1186/s12888-016-0928-0

Appendix

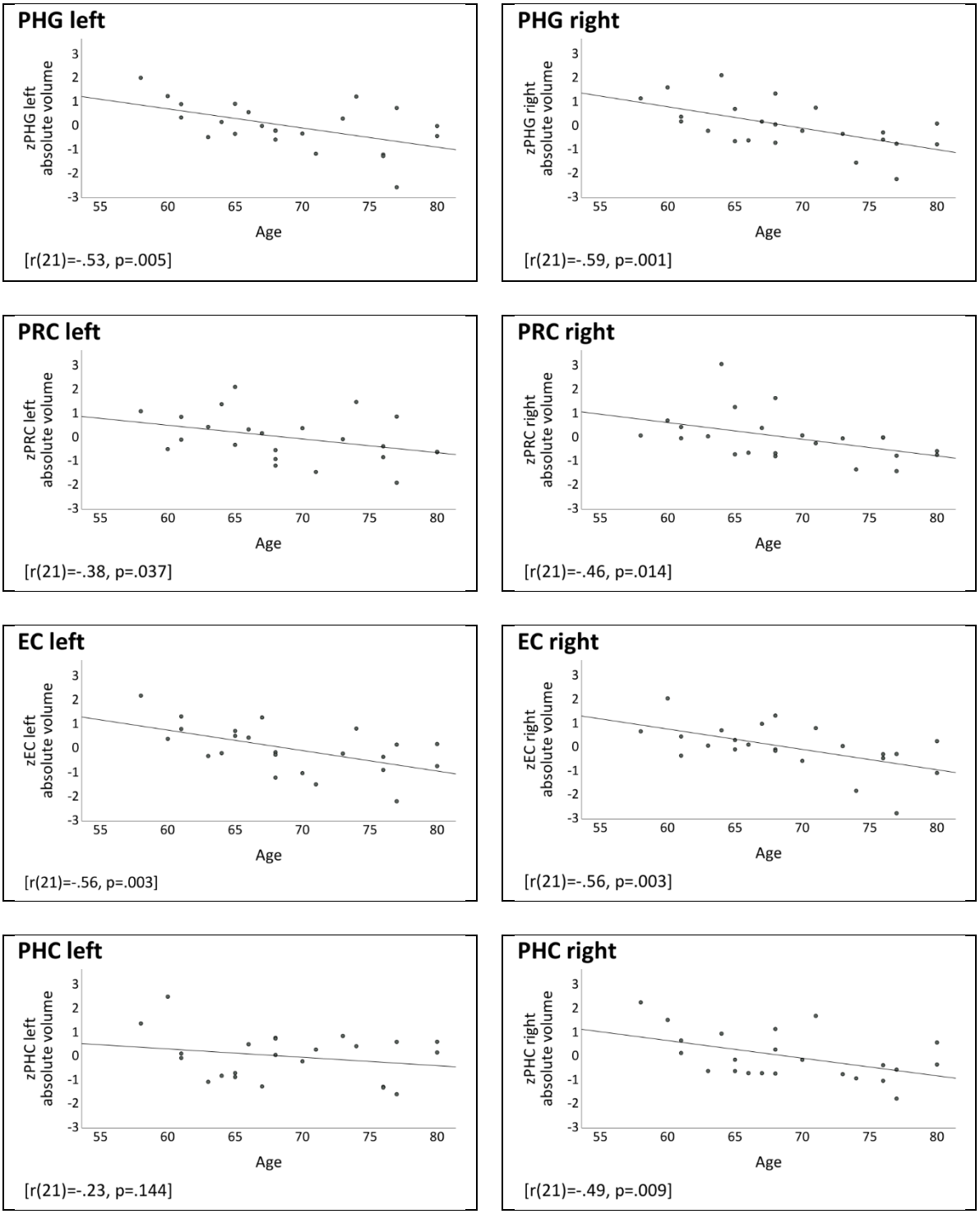

Appendix Figure A.1. Checking the linear relationship between age and the absolute integrity measurement in Scatterplots. Scatterplots are separated by hemisphere and parahippocampal structure. Each point represents a z-transformed value of the absolute cortical volume. The solid line represents the regression line with a linear slope that best fits the data points and was computed using the least squares method. Respective Pearson correlation coefficients are presented in square brackets. PHG=total parahippocampal gyrus; PRC=perirhinal cortex; EC=entorhinal cortex; PHC=parahippocampal cortex.

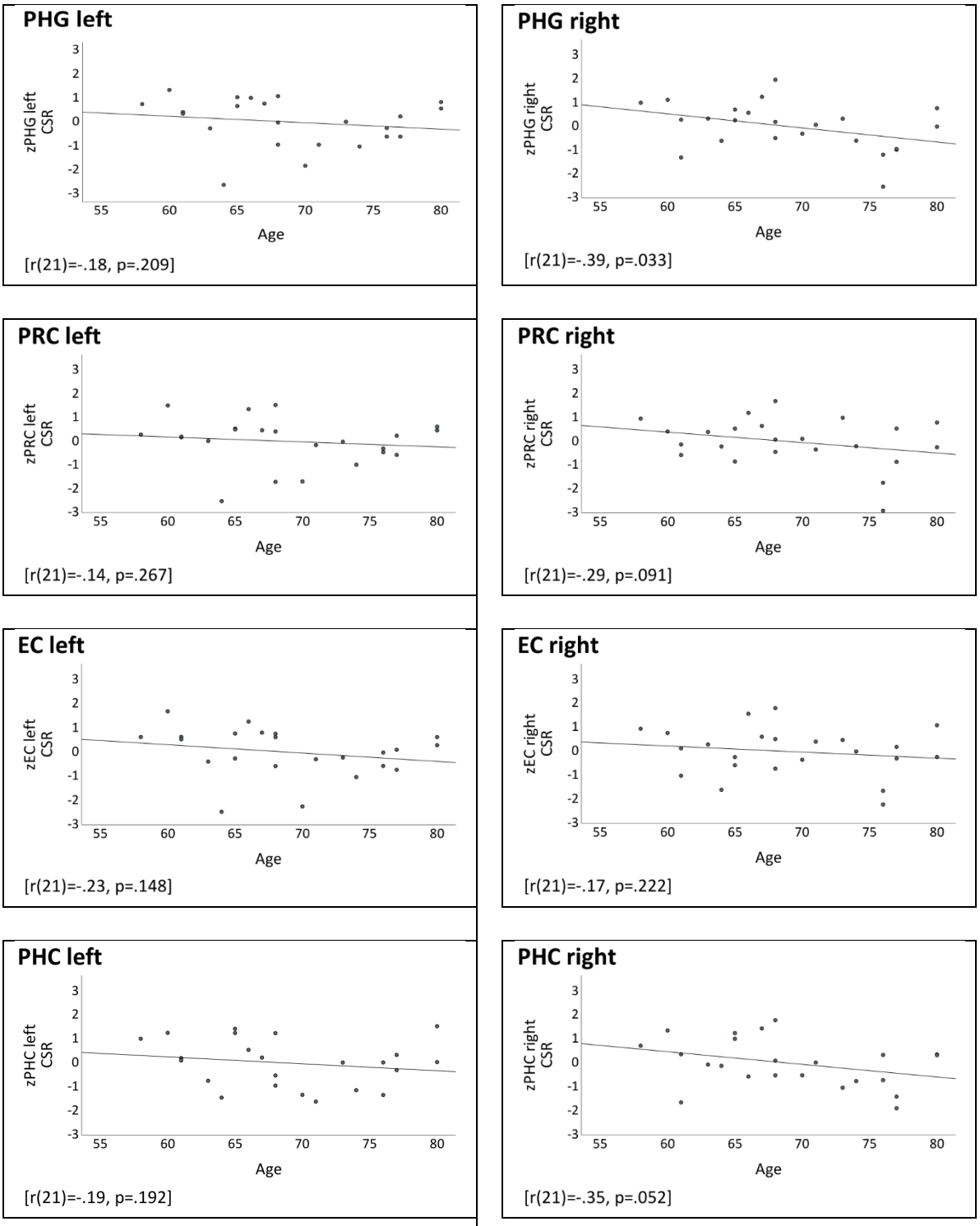

Appendix Figure A.2. Checking the linear relationship between age and the relative integrity measurement in Scatterplots. Scatterplots are separated by hemisphere and parahippocampal structure. Each point represents a z-transformed value of the CSR. The solid line represents the regression line with a linear slope that best fits the data points and was computed using the least squares method. Respective Pearson correlation coefficients are presented in square brackets. PHG=total parahippocampal gyrus; PRC=perirhinal cortex; EC=entorhinal cortex; PHC=parahippocampal cortex; CSR=Cortex-to-Sulcus-Ratio.

Appendix Table A

Mean, SD, minimum and maximum values for all examined structures separated by integrity measurement and hemisphere

		Uncorrected cortical volume [a]		Uncorrected sulcal volume [a]		Absolute cortical volume [a, b]		Absolute sulcal volume [a, b]		CSR [c]	
		left	right	left	right	left	right	left	right	left	right
Total parahippocampal gyrus (PHG)											
overall (*N*=23)	Mean	3646.91	3500.57	1205.09	1269.39	93.38	90.72	30.87	33.01	.75	.73
	SD	589.47	708.78	337.30	295.84	12.28	15.21	7.75	7.18	.04	.03
	Min	2217.00	2157.00	903.00	870.00	61.95	56.95	22.60	22.70	.64	.65
	Max	4494.00	5051.00	2238.00	2039.00	118.26	123.20	54.59	49.73	.81	.80
AD (*n*=8)	Mean	3118.63	3254.50	1169.00	1287.25	82.30	87.64	30.89	34.78	.73	.72
	SD	614.24	728.01	310.53	321.78	10.19	16.28	6.40	8.25	.03	.04
	Min	2217.00	2278.00	903.00	974.00	61.95	56.95	23.44	24.35	.67	.65
	Max	3834.00	4794.00	1795.00	1898.00	93.51	111.49	43.78	47.68	.79	.78
MCI (*n*=7)	Mean	3986.14	3482.29	1405.00	1340.43	102.21	91.01	35.85	34.93	.74	.72
	SD	307.43	894.33	442.78	397.38	9.73	19.17	10.37	8.27	.05	.03
	Min	3699.00	2157.00	1037.00	870.00	88.30	67.41	23.57	27.19	.64	.69
	Max	4494.00	5051.00	2238.00	2039.00	118.26	123.20	54.59	49.73	.79	.77
CN (*n*=8)	Mean	3878.38	3762.63	1066.25	1189.38	96.74	93.55	26.50	29.57	.78	.76
	SD	372.16	464.01	172.10	153.09	7.62	11.28	3.01	3.79	.02	.02
	Min	3271.00	3183.00	904.00	908.00	87.73	81.10	22.60	22.70	.74	.74
	Max	4354.00	473.00	1351.00	1394.00	108.85	115.41	30.70	34.00	.81	.80
Perirhinal cortex (PRC)											
overall (*N*=23)	Mean	1158.65	1114.09	612.09	640.83	53.73	51.22	28.24	29.39	.66	.64
	SD	268.35	334.08	282.33	252.13	10.45	13.59	11.86	10.47	.06	.05
	Min	580.00	562.00	301.00	329.00	33.95	32.10	15.05	15.61	.50	.50
	Max	1747.00	2050.00	1561.00	1203.00	75.96	93.18	67.87	54.68	.76	.72
AD (*n*=8)	Mean	978.88	1090.88	583.75	708.63	45.87	51.01	27.29	32.84	.63	.62
	SD	257.59	340.70	224.29	312.47	8.22	11.93	8.96	11.97	.05	.06
	Min	580.00	674.00	307.00	337.00	33.95	32.10	19.86	16.05	.55	.50
	Max	1336.00	1771.00	1020.00	1186.00	57.86	73.79	46.36	51.57	.69	.67
MCI (*n*=7)	Mean	1293.43	1132.14	770.71	642.14	61.34	52.72	36.02	29.85	.64	.64
	SD	200.25	455.64	390.40	281.68	8.12	19.65	15.98	12.15	.07	.03
	Min	1068.00	562.00	482.00	329.00	47.48	33.06	20.96	19.35	.50	.60
	Max	1573.00	2050.00	1561.00	1203.00	69.36	93.18	67.87	54.68	.69	.69
CN (*n*=8)	Mean	1220.50	1121.50	501.63	571.88	54.92	50.12	22.38	25.53	.71	.67
	SD	257.16	236.09	171.89	153.15	9.44	10.19	6.50	6.62	.04	.04
	Min	965.00	894.00	301.00	359.00	47.38	40.65	15.05	15.61	.67	.60
	Max	1747.00	1579.00	762.00	790.00	75.96	68.65	33.13	34.35	.76	.72
Entorhinal cortex (EC)											
overall (*N*=23)	Mean	790.30	766.96	496.35	533.04	44.74	43.24	27.91	29.85	.62	.60
	SD	207.71	189.55	243.66	226.16	10.39	9.39	12.38	11.37	.09	.08
	Min	323.00	294.00	219.00	216.00	22.06	17.29	13.50	12.71	.39	.43
	Max	1163.00	1116.00	1270.00	1025.00	67.56	62.59	66.84	54.94	.78	.74
AD (*n*=8)	Mean	669.13	723.25	466.63	588.63	38.22	42.00	26.79	33.44	.59	.56
	SD	263.16	246.26	209.78	291.95	10.75	12.06	10.23	13.55	.09	.08
	Min	323.00	294.00	219.00	216.00	22.06	17.29	17.71	12.71	.41	.43
	Max	1163.00	1116.0	881.00	1025.00	58.15	55.80	48.94	53.95	.70	.65
MCI (*n*=7)	Mean	856.86	712.43	629.14	523.43	49.80	40.48	35.65	29.71	.59	.59
	SD	128.13	183.69	324.43	234.80	10.62	8.60	16.22	12.49	.10	.07
	Min	707.00	366.00	379.00	245.00	37.21	26.14	19.95	17.50	.39	.48
	Max	1081.00	900.00	1270.00	989.00	67.56	50.00	66.84	54.94	.68	.67
CN (*n*=8)	Mean	853.25	858.38	409.88	485.88	46.84	46.91	22.26	26.39	.68	.65
	SD	162.90	92.96	158.66	148.65	6.91	6.58	7.32	7.77	.07	.07
	Min	516.00	754.00	240.00	287.00	32.25	42.47	13.50	15.11	.59	.56
	Max	1064.00	1064.00	666.00	703.00	53.20	62.59	35.05	37.00	.78	.74
Parahippocampal cortex (PHC)											
overall (*N*=23)	Mean	1697.96	1619.52	593.00	628.57	96.86	95.94	34.03	37.35	.74	.72
	SD	328.00	353.89	112.05	135.54	14.55	15.25	6.32	6.36	.03	.03
	Min	1175.00	994.00	379.00	414.00	73.78	68.95	23.56	25.88	.69	.66
	Max	2402.00	2387.00	783.00	940.00	133.44	130.60	45.85	49.47	.79	.78
AD (*n*=8)	Mean	1470.63	1440.38	585.25	578.63	88.64	90.75	35.40	36.37	.72	.71
	SD	271.00	303.44	134.08	142.84	12.98	15.68	7.84	7.16	.02	.03
	Min	1175.00	994.00	411.00	414.00	73.78	68.95	26.53	25.88	.69	.67
	Max	1858.00	1907.00	775.00	808.00	107.81	121.93	45.85	47.43	.75	.77
MCI (*n*=7)	Mean	1835.86	1637.71	634.29	698.29	102.25	97.74	35.48	41.83	.74	.70
	SD	220.66	381.80	84.16	141.43	10.23	17.42	5.26	5.77	.03	.03
	Min	1531.00	1225.00	526.00	541.00	85.06	81.93	26.43	33.55	.69	.66
	Max	2107.00	2101.00	783.00	940.00	117.06	130.60	43.50	49.47	.79	.74
CN (*n*=8)	Mean	1804.63	1782.75	564.63	617.50	100.37	99.54	31.39	34.40	.76	.74
	SD	363.13	330.32	112.78	111.10	16.95	13.26	5.31	4.00	.03	.03
	Min	1349.00	1408.00	379.00	443.00	81.35	85.28	23.56	28.44	.72	.70
	Max	2402.00	2387.00	674.0	771.00	133.44	119.35	37.44	39.00	.79	.78

Notes. [a] Uncorrected and absolute volumes are given in mm^3. [b] Absolute volumes were determined by dividing the uncorrected volumes by the number of labelled slices and operationalised the absolute measurement of parahippocampal integrity. [c] Cortex-to-Sulcus-Ratio (CSR) operationalised the relative measurement of parahippocampal integrity. AD=Alzheimer's disease; MCI=mild cognitive impairment; CN=cognitively normal.